Automatica 157 (2023) 111227

Contents lists available at ScienceDirect

Automatica

journal homepage: www.elsevier.com/locate/automatica

Model reduction by moment matching with preservation of global stability for a class of nonlinear models ☆

Mohammad Fahim Shakib [b,a,*], Giordano Scarciotti [b], Alexander Yu. Pogromsky [a], Alexey Pavlov [c], Nathan van de Wouw [a]

[a] Department of Mechanical Engineering, Eindhoven University of Technology, Eindhoven, The Netherlands
[b] Department of Electrical and Electronic Engineering, Imperial College London, London, UK
[c] Department of Geoscience and Petroleum, NTNU, Trondheim, Norway

ARTICLE INFO

Article history:
Received 28 March 2022
Received in revised form 27 March 2023
Accepted 1 June 2023
Available online 19 August 2023

Keywords:
Model order reduction
Moment matching
Nonlinear models
Convergent models
Lur'e-type models

ABSTRACT

Model reduction by time-domain moment matching naturally extends to nonlinear models, where the notion of moments has a local nature stemming from the center manifold theorem. In this paper, the notion of moments of nonlinear models is extended to the global case and is, subsequently, utilized for model order reduction of convergent Lur'e-type nonlinear models. This model order reduction approach preserves the Lur'e-type model structure, inherits the frequency-response function interpretation of moment matching, preserves the convergence property, and allows formulating a posteriori error bound. By the grace of the preservation of the convergence property, the reduced-order Lur'e-type model can be reliably used for generalized excitation signals without exhibiting instability issues. In a case study, the reduced-order model accurately matches the moment of the full-order Lur'e-type model and accurately describes the steady-state model response under input variations.

© 2023 The Authors. Published by Elsevier Ltd. This is an open access article under the CC BY license (http://creativecommons.org/licenses/by/4.0/).

1. Introduction

High-fidelity dynamical models of systems are essential in many engineering applications for analysis, prediction, and control design. Such models are typically described by a large number of coupled first-order differential equations, making model simulation computationally expensive and, sometimes, even infeasible due to limited computational and data storage capabilities. To reduce the computational cost and make model simulation feasible, the full-order model is replaced by a reduced-order model that resembles the behavior of the full-order model and preserves some key properties of the full-order model, e.g., stability properties. Techniques for finding a reduced-order model from a full-order model are called model order reduction techniques.

For the class of linear time-invariant (LTI) models, several reduction methods such as balanced truncation (Moore, 1981), Hankel-norm approximations (Glover, 1984), and the interpolation approach (Gallivan, Vandendorpe, & Van Dooren, 2004) have been proposed in the literature. However, most systems are essentially nonlinear and their models are, consequently, nonlinear too. The moment matching approach for LTI models, which belongs to the class of the interpolation approaches, has a natural extension to nonlinear models. Moments of LTI models are defined as the coefficients of the Laurent series expansion of the transfer function at a complex interpolation point, see Antoulas (2005), and the reduction method aims to match the moments of the reduced-order model to those of the full-order model. In Astolfi (2007), a time-domain interpretation of moment matching is given, which has naturally led to the definition of moments for nonlinear models consistent with the one for LTI models, and to reduced-order nonlinear models that achieve moment matching (Astolfi, 2010; Scarciotti & Astolfi, 2017a, 2017b). In these works, the definition of moments for nonlinear models makes use of the center manifold theorem and is, therefore, defined only locally in the neighborhood of the origin. Consequently, the formulated reduced-order model is by definition only an approximation of the full-order model in the neighborhood of the origin. In general, an estimate of the size of the neighborhood of the origin is lacking, an error bound is lacking as well and, by the same token, the reduction methods do not preserve the model structure of the full-order model.

Reduction methods that do preserve a global form of nonlinear model stability, e.g., incremental stability, and are equipped with error bounds, have also been proposed in the literature. The

☆ The material in this paper was partially presented at the 2021 American Control Conference (ACC), May 25–28, 2021, Virtual USA. This paper was recommended for publication in revised form by Associate Editor Aneel Tanwani under the direction of Editors Daniel Liberzon, Luca Zaccarian.

* Corresponding author.
E-mail addresses: m.shakib@imperial.ac.uk, m.f.shakib@tue.nl (M.F. Shakib), g.scarciotti@imperial.ac.uk (G. Scarciotti), a.pogromski@tue.nl (A.Y. Pogromsky), alexey.pavlov@ntnu.no (A. Pavlov), n.v.d.wouw@tue.nl (N. van de Wouw).

https://doi.org/10.1016/j.automatica.2023.111227
0005-1098/© 2023 The Authors. Published by Elsevier Ltd. This is an open access article under the CC BY license (http://creativecommons.org/licenses/by/4.0/).

methods in Besselink, van de Wouw, Scherpen, and Nijmeijer (2014), Kawano (2021), Kawano and Scherpen (2016, 2017) and Sarkar and Scherpen (2022) use generalized and extended differential balancing to truncate less important states of a nonlinear model, thereby preserving model stability and providing error bounds at the expense of losing model structure. Structure- and stability-preserving approaches have been proposed in Besselink, van de Wouw, and Nijmeijer (2011, 2013) and Padoan, Forni, and Sepulchre (2021) for nonlinear models that can be decomposed into a feedback interconnection of an LTI block with a static or dynamic nonlinear block. These methods reduce the state dimension of the LTI block using balanced truncation, formulate conditions for stability preservation (convergence in Besselink et al. (2011), incremental stability in Besselink et al. (2013), and dominance in Padoan et al. (2021)), and provide a priori error bounds. By employing bounded real balancing (Opdenacker & Jonckheere, 1988), the method in Besselink et al. (2013) provides a priori guaranteed stability preservation at the expense of accuracy. The methods in Besselink et al. (2013) and Padoan et al. (2021) preserve the stability property only if the reduction error is sufficiently small, thus prohibiting the reduction to an arbitrarily small order. The work in Padoan (2023) introduces an approximate moment matching framework in which an excessive number of moments are approximated. It is an open problem how this framework can be used to construct structure- and stability-preserving reduced-order nonlinear models. Although most of the above methods provide error bounds, in general, these error bounds cannot be trivially influenced in any way other than the order selection for the reduced-order model.

In this paper, the notion of moment of a nonlinear model is extended from the local context, as in Astolfi (2010) and Scarciotti and Astolfi (2017a, 2017b), to the global context for convergent nonlinear models. Hereto, the *local* center manifold theorem used in Astolfi (2010) and Scarciotti and Astolfi (2017a, 2017b) is replaced with a *global* invariant manifold result from Pavlov, van de Wouw, and Nijmeijer (2006). Convergent nonlinear models exhibit a strong form of model stability; namely, for any bounded input, a convergent model exhibits a bounded and globally asymptotically stable steady-state solution, implying that the effect of the initial condition fades out. Using the proposed global notion of moments, a constructive reduction method for the class of convergent Lur'e-type models is presented. Lur'e-type models, see Fig. 1, consist of LTI dynamics placed in feedback with a static nonlinearity, and arise naturally in problems with localized nonlinearities (Khalil, 1996), making them practically relevant.

The reduction method for Lur'e-type models only reduces the state dimension of the LTI block and inherits the static nonlinearity of the full-order model, which preserves the Lur'e-type model structure. A benefit of such structure preservation is that it also preserves the physical interpretation of the Lur'e-type model. In addition, a rich array of analysis and design tools are available for the class of Lur'e-type models, see, e.g., Khalil (1996), which are then compatible with the reduced-order model. To achieve moment matching and to preserve the Lur'e-type model structure including the static nonlinearity, the transfer function of the LTI dynamics should match at an infinite number of interpolation points, which is generally not possible when the model order is reduced. Therefore, the proposed reduction methodology matches the transfer function only at a finite number of interpolation points, thereby *approximating* the moment of the full-order model. The proposed reduction method enjoys several benefits besides (Lur'e-type) structure preservation: namely, it preserves the convergence property (which implies preservation of global, as opposed to local, stability properties), it inherits the FRF interpretation of moment matching, it provides a computable a posteriori error bound, and it enables reduction of this error

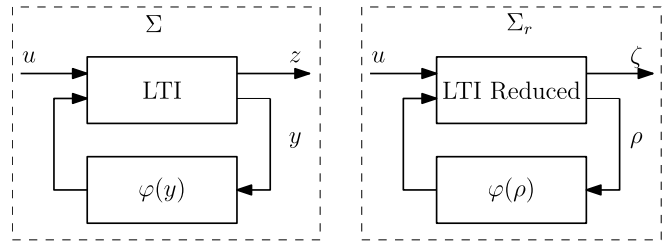

Fig. 1. Full-order (left) and reduced-order (right) Lur'e-type model. Only the dimension of the LTI block is reduced.

bound. This error bound is on the L_2-norm of the difference between the moment of the full-order and reduced-order models and also generalizes to the steady-state mismatch between the responses of the full-order and reduced-order Lur'e-type models for generalized periodic inputs. By solving an optimization problem, the proposed approach aims to find the reduced-order model that minimizes the error bound and hence the reduction error.

To summarize, the main contributions of this paper are (i) the extension of the notion of moments to the global case for a generic class of convergent nonlinear models; and (ii) a constructive model order reduction approach for convergent Lur'e-type models that preserves the convergence property in addition to preserving the Lur'e-type model structure. Furthermore, this reduction approach has an FRF interpretation and is equipped with a corresponding error bound that is minimized. The methods developed in this paper are quantitatively analyzed in a case study on a flexible beam.

A preliminary part of the reduction method in this paper has been presented in Shakib, Scarciotti, Pogromsky, Pavlov, and van de Wouw (2021). Compared to Shakib et al. (2021), the current paper considers an extended class of Lur'e-type models and includes the definition of moments of generic nonlinear convergent models in the global context. Furthermore, this paper provides an error bound for the reduction method for Lur'e-type models and includes a novel numerical case study.

The remainder of this paper is structured as follows. The end of Section 1 introduces the notation used throughout the rest of this paper. Section 2 extends the notion of moments to the global case for generic convergent nonlinear models and formally introduces the model order reduction problem for convergent Lur'e-type models. Section 3 proposes an approach to the model order reduction of Lur'e-type models. Section 4 describes the results of a case study that illustrates the application and benefits of the proposed model-order reduction approach. Section 5 gives the concluding remarks.

Notation and preliminaries Throughout this paper, the following notation is used. By $\mathbb{Z}, \mathbb{Z}_{\geq 0}\mathbb{R}, \mathbb{R}_{\geq 0}, \mathbb{C}, \mathbb{C}^0, \mathbb{C}^-$ we, respectively, denote the set of integers, non-negative integers, real numbers, non-negative real numbers, complex numbers, complex numbers with zero real part and complex numbers with a negative real part. For a vector $x \in \mathbb{R}^n$, we denote the Euclidean norm by $|x| := \sqrt{x^\top x}$. The set of eigenvalues of a matrix $A \in \mathbb{R}^{n\times n}$ is denoted by $\sigma(A)$ and the matrix A is positive (negative) definite, denoted by $A \succ 0 (A \prec 0)$, if all its eigenvalues are positive (negative). A continuous function $\alpha : [0, a) \to [0, +\infty)$ is said to belong to class $\mathcal{K}$ if it is strictly increasing and $\alpha(0) = 0$. It is said to belong to class $\mathcal{K}_\infty$ if $a = +\infty$ and $\alpha(r) \to +\infty$ as $r \to +\infty$. A continuous function $\beta : [0, a) \times [0, +\infty) \to [0, +\infty)$ is said to belong to class $\mathcal{KL}$ if, for each fixed s, the mapping $\beta(r, s)$ belongs to class $\mathcal{K}$ with respect to r and, for each fixed r, the mapping $\beta(r, s)$ is decreasing with respect to s and $\beta(r, s) \to 0$ as $s \to \infty$. By $L_2(T)$ we denote the space of continuous real-valued T-periodic scalar functions $y(t)$ satisfying $\|y\|_{L_2} < +\infty$, where $\|y\|_{L_2}^2 := \frac{1}{T}\int_0^T |y(t)|^2 dt$ is the L_2-norm.

2. Problem statement

Consider a single-input, single-output (SISO), continuous-time minimal nonlinear model described by the equations

$$\dot{x} = f(x, u), \quad y = h(x) \tag{1}$$

with $x(t) \in \mathbb{R}^n, u(t) \in \mathbb{R}, y(t) \in \mathbb{R}$, the mapping f locally Lipschitz in x and continuous in u and the mapping h locally Lipschitz in x. Moments of the nonlinear model (1) are defined in the literature based on the existence of a solution to a partial differential equation (PDE) which characterizes a center manifold that is only defined locally. In this paper, based on the stability notion of convergence, we introduce in Section 2.1 a global invariant manifold theorem (Pavlov et al., 2006) that replaces the center manifold theorem, thereby allowing for defining moments in a global context for the generic class of convergent nonlinear models.

After that, Section 2.2 presents tractable conditions for convergence of Lur'e-type models under which moments are well-defined. A Lur'e-type model consists of a static nonlinear block placed in feedback with an LTI block, see Fig. 1, and is described by the following state–space equations:

$$\Sigma : \begin{array}{ll} \dot{x} & = Ax + B_1 u + B_2 \varphi(y), \\ y & = C_1 x, \\ z & = C_2 x, \end{array} \tag{2}$$

where $x(t) \in \mathbb{R}^n$ is the state, $u(t) \in \mathbb{R}$ is the input, $y(t) \in \mathbb{R}$ is the input to the nonlinear mapping $\varphi : \mathbb{R} \to \mathbb{R}$, $z(t) \in \mathbb{R}$ is the output and model matrices $A \in \mathbb{R}^{n\times n}$, $B_1, B_2 \in \mathbb{R}^{n\times 1}$, $C_1, C_2 \in \mathbb{R}^{1\times n}$.

Subsequently, Section 2.3 introduces the problem of finding a reduced-order model for (2) that achieves moment matching. Here, the class of reduced-order models Σ_r of order ν is defined as follows:

$$\Sigma_r : \begin{array}{ll} \dot{\xi} & = F\xi + G_1 u + G_2 \varphi(\rho), \\ \rho & = H_1 \xi, \\ \zeta & = H_2 \xi, \end{array} \tag{3}$$

where $\xi(t) \in \mathbb{R}^\nu$ is the state, $u(t) \in \mathbb{R}$ is the input, $\rho(t) \in \mathbb{R}$ is the input to the same nonlinear mapping $\varphi : \mathbb{R} \to \mathbb{R}$ as in (2), $\zeta(t) \in \mathbb{R}$ is the output and the model matrices are $F \in \mathbb{R}^{\nu\times\nu}$, $G_1, G_2 \in \mathbb{R}^{\nu\times 1}$, $H_1, H_2 \in \mathbb{R}^{1\times\nu}$. In this problem, the Lur'e-type model structure, the nonlinear mapping φ, and the convergence property of the full-order model Σ in (2) are preserved for the reduced-order model Σ_r in (3). As is detailed in Section 2.3, in general, it is not possible to exactly match the moment of Σ in (2) in this problem, hence leading to the notion of *approximate moment matching* problem. Finally, Section 2.4 formalizes the approximate moment matching problem as a constrained optimization problem.

2.1. Moments of generic nonlinear models

Consider a signal generator described by the equations

$$\dot{\tau} = s(\tau), \quad u = l(\tau) \tag{4}$$

with $\tau(t) \in \mathbb{R}^\nu$, the mappings s and l locally Lipschitz in τ and we assume that the solutions of (4) exist on the whole time axis $\mathbb{R}$, which is the case, e.g., if s is globally Lipschitz in τ. Moreover, consider its interconnection with (1), defined as follows:

$$\dot{\tau} = s(\tau), \quad \dot{x} = f(x, l(\tau)), \quad y = h(x). \tag{5}$$

Prior to defining the moments, we define the notion of observability.

Definition 1 (*Scarciotti & Astolfi, 2017b*)**.** The signal generator (4), characterized by the pair (s, l), is observable if for any pair of initial conditions $\tau_a(0) \in \mathbb{R}^\nu$ and $\tau_b(0) \in \mathbb{R}^\nu$, such that $\tau_a(0) \neq \tau_b(0)$, the corresponding output trajectories $l(\tau_a(t))$ and $l(\tau_b(t))$ are such that $l(\tau_a(t)) - l(\tau_b(t)) \not\equiv 0$.

Definition 2. Consider the interconnected model (5) and suppose that the pair (s, l) is observable according to Definition 1. Suppose there exists a unique function $\pi : \mathbb{R}^\nu \to \mathbb{R}^n : \tau \mapsto \pi(\tau)$ such that the graph

$$\mathcal{M} := \{(\tau, x) : x = \pi(\tau), \tau \in \mathbb{R}^\nu\} \tag{6}$$

is invariant with respect to the interconnected model (5). Then, the function $h \circ \pi$ is called the moment of the model (1) at (s, l).

The definition of moments in Definition 2 is consistent with its counterpart for LTI models (Scarciotti & Astolfi, 2017b), though different from Astolfi (2010) and Scarciotti and Astolfi (2017a, 2017b), see Remark 6. Different types of sufficient conditions are formulated in the literature for the function π to exist and be unique, see, e.g., Isidori, Sontag, and Thoma (1995) and Khalil (1996). In the scope of this work, we pose two assumptions that guarantee the existence and uniqueness of π.

Assumption 1. For any $a > 0$, there exists a $b > 0$ such that the initial condition $|\tau(0)| \leq a$ implies that the state evolution $\tau(t) \in \mathbb{R}^\nu$ of the signal generator (4) satisfies $|\tau(t)| \leq b$ for all $t \in (-\infty, \infty)$. Furthermore, the signal generator (4) is observable according to Definition 1.

Next, we pose an assumption on the stability properties of the nonlinear model (1). Hereto, define $\mathcal{U}$ as the set of piecewise-continuous functions $u(t) \in \mathbb{R}$ that are defined and bounded on $t \in \mathbb{R}$.

Definition 3 (*Pavlov et al., 2006*)**.** The model (1) is said to be globally (uniformly, exponentially) convergent if for every input $u \in \mathcal{U}$, there exists a solution $\bar{x}_u$ to (1) satisfying the following conditions:

- $\bar{x}_u$ is defined and bounded on $t \in \mathbb{R}$,
- $\bar{x}_u$ is globally (uniformly asymptotically, exponentially) stable.

The solution $\bar{x}_u$ is called the steady-state solution. The notion of input-to-state convergence is an even stronger stability property and is defined as follows.

Definition 4 (*Pavlov et al., 2006*)**.** Model (1) is said to be input-to-state convergent if it is globally uniformly convergent for the class of inputs $\mathcal{U}$ and for every input $u \in \mathcal{U}$, model (1) is input-to-state stable with respect to the steady-state solution $\bar{x}_u(t)$, i.e., there exist a $\mathcal{KL}$-function $\beta(r, s)$ and a $\mathcal{K}_\infty$-function $\gamma(r)$ such that any solution $x(t)$ of model (1) corresponding to some input $\hat{u}(t) := u(t) + \Delta u(t)$ satisfies

$$|x(t) - \bar{x}_u(t)| \leq \beta(|x(t_0) - \bar{x}(t_0)|, t - t_0) + \gamma\left(\sup_{t_0 \leq \tau \leq t} |\Delta u(\tau)|\right) \tag{7}$$

for all $t, t_0 \in \mathbb{R}$, $t \geq t_0$. The functions $\beta(r, s)$ and $\gamma(r)$ may depend on the particular input u.

Convergent models forget their initial condition and converge to the uniquely defined steady-state solution $\bar{x}_u$. In addition, as evidenced from (7), input-to-state convergent models are robust against input variations, because the steady-state difference $|x(t) - \bar{x}_u(t)|$ increases monotonically with $|\Delta u(t)|$, implying that small values $|\Delta u(t)|$ result in small steady-state values $|x(t) - \bar{x}_u(t)|$.

Assumption 2. The model (1) is input-to-state convergent according to Definition 4.

Assumptions 1 and 2 guarantee the existence of a *globally* asymptotically stable invariant manifold. This invariant manifold is the counterpart of the center manifold used in previous literature (Astolfi, 2010; Scarciotti & Astolfi, 2017a, 2017b).

Lemma 5 (Pavlov et al., 2006). *Under Assumptions 1 and 2, there exists a unique, continuous function π as in Definition 2, such that the graph $\mathcal{M}$ in (6) is invariant with respect to the interconnected model (5). Moreover, for every input $u(t)$ generated by (4), the corresponding steady-state solution of (5) is given by $\bar{x}_u(t) = \pi(\tau(t))$ and is globally uniformly asymptotically stable. Furthermore, if $\pi(\tau)$ is continuously differentiable, i.e., $\pi(\tau) \in C^1$, then $\pi(\tau)$ solves the partial differential equation*

$$\frac{\partial \pi(\tau)}{\partial \tau} s(\tau) = f(\pi(\tau), l(\tau)), \quad \tau(t) \in \mathbb{R}^{\nu}. \tag{8}$$

Lemma 5 guarantees that moment $h \circ \pi$, see Definition 2, is well-defined (also *non-locally*) for nonlinear models that enjoy the input-to-state convergence property. Furthermore, since the graph $\mathcal{M}$ in (6) is described by the globally asymptotically stable steady-state solution $\bar{x}_u$, it can be found by computer simulation of the dynamics of the interconnected dynamics (5). For example, the graph $\mathcal{M}$ can be computed efficiently using the so-called MTF simulation algorithm (Pavlov, Hunnekens, van de Wouw, & Nijmeijer, 2013) for the class of Lur'e-type models. Remark 7 comments on finding reduced-order models that preserve the convergence property. The notion of a moment of a nonlinear model in a global context is employed in the remainder of this paper to devise a numerically tractable reduction approach for the class of convergent Lur'e-type models.

Remark 6. The notion of a moment of nonlinear models has been introduced in Astolfi (2010), see also Scarciotti and Astolfi (2017a, 2017b), based on the solution of the PDE (8), given that $\pi(\tau)$ is C^1 in the neighborhood of the origin (under certain assumptions). In our paper, however, Assumptions 1 and 2 do not guarantee that $\pi(\tau)$ is C^1, but only guarantee that the invariant manifold described by the graph $\mathcal{M}$ in (6) exists, is unique and continuous. Therefore, the notion of a moment as in Definition 2, is solely based on $\mathcal{M}$ in (6). A definition of moments based on a similar invariant set as in (6) was introduced in Scarciotti, Teel, and Astolfi (2017) for linear differential inclusions.

Remark 7. Combining the results in Scarciotti and Astolfi (2017b) with the insight that the convergence property allows for the well-defined global definition of moments (as in Definition 2 of the current paper), an extension towards a family of reduced-order models can be formulated that achieves moment matching in the global context. To preserve convergence, the reduced-order model should satisfy conditions for convergence, e.g., the so-called Demidovich's condition resulting in input-to-state convergence, see Pavlov et al. (2006, Theorem 2.29).

2.2. Moments of convergent Lur'e-type models

Consider a Lur'e-type model Σ in (2) and denote by $\Phi_{(i,k)}(j\omega)$, $i, k \in \{1, 2\}$ the FRF associated to its LTI part, which is defined as follows:

$$\Phi_{(i,k)}(j\omega) := C_i(j\omega I - A)^{-1}B_k, \text{ for } i, k \in \{1, 2\}. \tag{9}$$

The following theorem presents conditions for the convergence of the Lur'e-type model (2).

Theorem 8 (Pavlov et al., 2006). *Consider model (2). Suppose that for some constant $\gamma > 0$ the nonlinear function φ satisfies the following incremental sector condition:*

$$|\varphi(y_2) - \varphi(y_1)| \leq \gamma |y_2 - y_1|, \quad \forall y_1, y_2 \in \mathbb{R}. \tag{10}$$

Denote $A_\gamma^- := A - \gamma B_2 C_1$ and $A_\gamma^+ := A + \gamma B_2 C_1$. If there exists a $P = P^\top \succ 0$ such that

$$PA_\gamma^- + (A_\gamma^-)^\top P \prec 0 \text{ and } PA_\gamma^+ + (A_\gamma^+)^\top P \prec 0 \tag{11}$$

hold, then model (2) is globally exponentially convergent according to Definition 3 and input-to-state convergent according to Definition 4.

From here onwards, we simply say that a model is *convergent* to imply that the model is both exponentially convergent according to Definition 3 and input-to-state convergent according to Definition 4. Since the dimension n of the full-order model is assumed large, it is not practical to solve the linear matrix inequalities (LMIs) in Theorem 8 to verify whether the full-order model is convergent. Alternatively, one can equivalently verify the following three conditions (see, e.g., Pavlov et al. (2006)): (1) the incremental sector condition (10); (2) the matrix A being Hurwitz, i.e., $\sigma(A) \in \mathbb{C}^-$; and (3) satisfaction of the following inequality:

$$\sup_{\omega \in \mathbb{R}} \left|\Phi_{(1,2)}(j\omega)\right| = \sup_{\omega \in \mathbb{R}} \left|C_1(j\omega I - A)^{-1}B_2\right| < \frac{1}{\gamma}. \tag{12}$$

Inequality (12) can be verified graphically, e.g., using the Bode magnitude plot of $\Phi_{(1,2)}(j\omega)$.

The reduction method to be presented in Section 3 inherits the FRF interpretation of LTI moment matching thanks to using linear signal generators:

$$\dot{\tau} = S\tau, \quad u = L\tau \tag{13}$$

with state $\tau(t) \in \mathbb{R}^{\nu}$, output $u(t) \in \mathbb{R}$ and matrices $S \in \mathbb{R}^{\nu \times \nu}$ and $L \in \mathbb{R}^{1 \times \nu}$. The next assumption guarantees the satisfaction of Assumption 1.

Assumption 3. The matrix S of (13) has simple eigenvalues that are located on the imaginary axis. In addition, the pair (S, L) is observable.

Finally, the next assumption guarantees the satisfaction of Assumption 2.

Assumption 4. The Lur'e-type model (2) satisfies the conditions of Theorem 8 for $\gamma = \gamma^\star$ for some $\gamma^\star > 0$ and is, therefore, convergent.

Because Assumptions 1 and 2 are implied by Assumptions 3 and 4, application of Lemma 5 guarantees that the moment of the Lur'e-type model is well-defined, i.e., it guarantees the existence of a globally exponentially stable invariant manifold described by $\bar{x}_u(t) = \pi(\tau(t))$ with $\pi : \mathbb{R}^{\nu} \to \mathbb{R}^n : \tau \mapsto \pi(\tau)$. The moment of the full-order model (2) at (S, L) is denoted by $C_2\pi$ with π as in Definition 2.

2.3. Approximate moment matching problem

Model order reduction of Lur'e-type models boils down to reducing the state dimension of the LTI block since all the dynamics are captured therein. Consequently, the proposed reduction method preserves the Lur'e-type structure of the full-order model and inherits the FRF interpretation that is characteristic of moment matching for LTI models. Solely reducing the dimension of the LTI block results inevitably in the moments of the full-order Lur'e-type model being approximated rather than being exactly matched, which is further explained below.

Consider the class of models Σ_r in (3). The moment of this model at (S, L) is denoted by $H_2 p$, where the function p plays the role of the function π in Definition 2. The FRFs associated with the LTI part of (3) read as:

$$\Gamma_{(i,k)}(j\omega) := H_i(j\omega I - F)^{-1}G_k \text{ for } i, k \in \{1, 2\}. \tag{14}$$

The main obstacle in achieving moment matching is that the steady-state output $\bar{z}_u$ of the full-order model, related to the moment via $\bar{z}_u = C_2\bar{x}_u = C_2\pi(\tau(t))$, typically consists of an infinite number of harmonics due to the nonlinear feedback φ. Therefore, to match the steady-state output $\bar{z}_u$ of the full-order model by the steady-state output $\bar{\zeta}_u$ of the reduced-order model, a match should be achieved between the FRFs of the LTI part of the full-order and the reduced-order models at an infinite number of interpolation frequencies. Even though some methods have been proposed to match moments at infinitely many interpolation points, see Scarciotti and Astolfi (2017b), these cannot be trivially generalized to the current setting without losing model structure. Therefore, in this work, only a finite number of interpolation frequencies are matched in each of the FRFs in (9), resulting inevitably in a mismatch in the nonlinear moment.

Having a mismatch between the moment of the full-order and of the reduced-order Lur'e-type model makes it particularly important to derive an error bound for this mismatch. Such error bound is an important part of the *approximate moment matching problem*, in addition to preserving the convergence property.

Problem 9. Consider the full-order Lur'e-type model (2) with state dimension n and the signal generator (13) with state $\tau(t) \in \mathbb{R}^{\nu}$ characterized by (S, L) and suppose $\nu < n$. Suppose Assumptions 3 and 4 hold for some $\gamma^\star > 0$. Denote the moment of the full-order Lur'e-type model (2) at (S, L) by $C_2\pi$.

The approximate moment matching problem is to find matrices F, G_1, G_2, H_1, H_2, which define the ν-th order model (3) with moment $H_2 p$, such that this reduced-order model satisfies the condition in Theorem 8, and to find a constant $0 \leq \varepsilon < +\infty$ such that the mismatch between the moment of the full-order and reduced-order Lur'e-type model is upper bounded as follows:

$$\|C_2\pi(\tau) - H_2 p(\tau)\|_{L_2} \leq \varepsilon \, \|L\tau\|_{L_2} \,. \tag{15}$$

This problem is further formalized in the next section.

Remark 10. Other methods, e.g., the method in Astolfi (2010), do achieve moment matching rather than approximate moment matching, for example, by considering a Wiener model, i.e., linear dynamics followed by a static nonlinear output map. However, in those methods, the model structure is generally not preserved. Furthermore, Lur'e-type models represent a broader model class than Wiener models do.

2.4. Constrained optimization problem formulation

Frequency-domain insights are used to formulate a constrained optimization problem, which, on the one hand, allows finding a constant ε to solve Problem 9 and, on the other hand, aims at reducing ε to improve the accuracy of the estimated reduced-order model. Let us first further motivate moment matching at a finite number of interpolation points by the following two properties.

Property 11 (*Pavlov et al., 2006*). *Consider the model (2) and suppose Assumption 4 holds. If the input $u \in L_2(T)$ is T-periodic, then the corresponding steady-state outputs $\bar{z}_u$ and $\bar{y}_u$ are also periodic with the same period T.*

Property 12. *Consider the model (2) and suppose Assumption 4 holds. If the input $u \in L_2(T)$ has a finite Lipschitz constant $0 \leq \ell < +\infty$ with respect to time t, i.e., $|u(t) - u(t+\kappa)| \leq \ell|\kappa| \, \forall \, t, \kappa \in \mathbb{R}$, then the magnitude of the kth Fourier coefficient of the Fourier series of $\bar{z}_u$ and $\bar{y}_u$ converges to zero according to $O(1/k)$ for $k \neq 0$.*

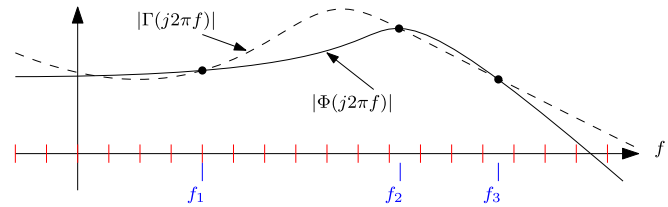

Fig. 2. The FRFs of the reduced-order and full-order model match at the frequencies in the set $\Omega^0 = \{f_1, f_2, f_3\}$. The mismatch between the FRFs is minimized at the frequencies in Ω^M, here taken on the red grid illustrated in the figure.

Proof. The input u having a finite Lipschitz constant results in each of the steady-state outputs $\bar{z}_u$ and $\bar{y}_u$ of model (2) also admitting a finite Lipschitz constant, possibly different from ℓ. The magnitude of the kth Fourier coefficient of a Lipschitz continuous function is of order $O(1/k)$ for $k \neq 0$, see, e.g., Katznelson (2004, Theorem 4.6). ■

Property 11 ensures that the signal $\varphi(\bar{y}_u)$ consists of the same frequencies as u and an infinite number of higher harmonic frequencies. Property 12 ensures that the Fourier coefficients of large frequencies vanish in absolute value, justifying matching only a finite number of frequencies in the corresponding FRFs (note that by Assumption 3, the output of the linear harmonic oscillator is Lipschitz continuous with respect to time, as required in Property 12). Considering these properties, for approximate moment matching, it is beneficial to match the involved FRFs of the LTI block of the Lur'e-type model at the first few harmonics and/or at frequencies corresponding to important model characteristics, such as the 0-Hz frequency or the (anti-) resonance peaks. Hereto, we collect $\eta_{(i,k)}$ user-defined interpolation frequencies in the vector $\Omega^0_{(i,k)} \in \mathbb{R}^{\eta_{(i,k)}}$ for each $i, k \in \{1, 2\}$, where indices i, k refer to the FRFs (9).

To achieve robustness against input variations, we also minimize the mismatch in these FRFs at other frequencies, which has two additional benefits. Firstly, it allows for reducing the mismatch at the harmonics and intermodulation frequencies that are not included as interpolation frequencies in $\Omega^0_{(i,k)}$, resulting in a better approximation of the moment of the Lur'e-type model. Secondly, it adds to the robustness of the reduced-order Lur'e-type model for new inputs that excite different frequencies than the interpolation frequencies. We collect $M_{(i,k)}$ user-defined frequencies in the vector $\Omega^M_{(i,k)} \in \mathbb{R}^{M_{(i,k)}}$ for each $i, k \in \{1, 2\}$, at which the mismatch in FRFs is minimized. An illustration of the sets Ω^0 and Ω^M for a single FRF is presented in Fig. 2.

Before formally presenting the constrained optimization problem, we define the mismatch in each FRF as follows:

$$\Upsilon_{(i,k)}(j\omega) := \Phi_{(i,k)}(j\omega) - \Gamma_{(i,k)}(j\omega), \, i, k \in \{1, 2\}, \tag{16}$$

where $\Phi_{(i,k)}(j\omega)$ and $\Gamma_{(i,k)}(j\omega)$, $i, k \in \{1, 2\}$, are defined in (9), (14), respectively. Furthermore, we define the cost function to be minimized:

$$J(F, G_1, G_2, H_1, H_2) := \sum_{k=1}^{2} \sum_{i=1}^{2} \sum_{\ell=1}^{M_{(i,k)}} \left| \Upsilon_{(i,k)}(j\omega_{(i,k)}(\ell)) \right|^2 , \tag{17}$$

where $\omega_{(i,k)}(\ell)$ is the ℓ-th component of $\Omega^0_{(i,k)}$ and $\Upsilon_{(i,k)}$ is defined in (16).

Problem 13. Consider the full-order Lur'e-type model (2) and suppose Assumption 4 holds for some $\gamma^\star > 0$. Furthermore, consider given sets of frequencies $\Omega^0_{(i,k)} \in \mathbb{R}^{\eta_i}$, $\Omega^M_{(i,k)} \in \mathbb{R}^{M_{(i,k)}}$ for $i, k \in \{1, 2\}$. The reduced-order model (3), characterized by

F, G_1, G_2, H_1, H_2 is found by solving the following constrained optimization problem:

$$\min_{F,G_1,G_2,H_1,H_2} J(F, G_1, G_2, H_1, H_2) \quad \text{subject to} \tag{18a}$$

$$\Upsilon_{(i,k)}(j\omega) = 0 \,\forall\, \omega \in \Omega^0_{(i,k)},\, i, k \in \{1, 2\}, \tag{18b}$$

$$Q = Q^\top \succ 0, \tag{18c}$$

$$QF^-_{\gamma^\star} + (F^-_{\gamma^\star})^\top Q \prec 0, \tag{18d}$$

$$QF^+_{\gamma^\star} + (F^+_{\gamma^\star})^\top Q \prec 0, \tag{18e}$$

where $F^-_{\gamma^\star} = F - \gamma^\star G_2 H_1$, $F^+_{\gamma^\star} = F + \gamma^\star G_2 H_1$ and $J(F, G_1, G_2, H_1, H_2)$ as defined in (17).

Problem 13 has the following interpretation. The minimization of $J(F, G_1, G_2, H_1, H_2)$ in (18a) ensures an optimal fit between the FRFs of the full-order and reduced-order model, for $i, k \in \{1, 2\}$, at the frequencies $\Omega^M_{(i,k)}$, for $i, k \in \{1, 2\}$. The constraint (18b) ensures that the FRF $\Phi_{(i,k)}$ of the full-order model equals the FRF $\Gamma_{(i,k)}$ of the reduced-order model at the interpolation frequencies Ω^i_0, $i = 1, 2$, for $i, k \in \{1, 2\}$. The remaining constraints (18c)–(18e) guarantee that the reduced-order Lur'e-type model (3) preserves the convergence property of the full-order Lur'e-type model (2) by satisfying the conditions of Theorem 8, guaranteeing that a constant ε exists to solve Problem 9. Moreover, it is shown in Section 3 that Problem 9 minimizes the constant ε in Problem 13.

Remark 14. For the sake of exposition, a frequency-dependent weighting in the cost function (17) is not introduced; one could trivially equip the cost function with such weighting. Weighting can be useful to emphasize the importance of a good fit for desired frequency ranges.

3. Solution to the approximate moment matching problem

First, a solution to Problem 13 is proposed in Section 3.1. After that, it is shown how this solution also solves Problem 9 in Section 3.2. An overview of the reduction method is presented in Section 3.3.

3.1. Solution to the optimization Problem 13

The proposed solution to Problem 13 works as follows. Firstly, by application of time-domain moment matching for LTI models, a family of Lur'e-type models (3) is derived such that constraint (18b) of Problem 13 is satisfied. As shown below, this step yields freedom in vectors G_1, G_2, which is exploited to solve the optimization problem (18a) while satisfying the constraints (18c)–(18e) in order to ensure the convergence property.

3.1.1. Family of reduced-order Lur'e-type models

Let us recall an adapted version of the time-domain moment matching method for SISO LTI models from Astolfi (2010). Consider a minimal LTI model described by:

$$\dot{x} = \mathcal{A}x + \mathcal{B}u, \qquad y = \mathcal{C}x, \tag{19}$$

where $x(t) \in \mathbb{R}^n$ is the state, $u(t) \in \mathbb{R}$ is the input, $y(t) \in \mathbb{R}$ the output and $\mathcal{A} \in \mathbb{R}^{n\times n}$, $\mathcal{B} \in \mathbb{R}^{n\times 1}$, $\mathcal{C} \in \mathbb{R}^{1\times n}$ are model matrices. Consider the reduced-order LTI model

$$\dot{\xi} = \mathcal{F}x + \mathcal{G}u, \qquad y = \mathcal{H}x, \tag{20}$$

where $\xi(t) \in \mathbb{R}^\nu$ is the state, $u(t) \in \mathbb{R}$ is the input, $y(t) \in \mathbb{R}$ the output and $\mathcal{F} \in \mathbb{R}^{\nu\times\nu}$, $\mathcal{G} \in \mathbb{R}^{\nu\times 1}$, $\mathcal{H} \in \mathbb{R}^{1\times\nu}$ are model matrices and $\nu < n$. The following theorem borrowed from Astolfi (2010) is specialized to simple interpolation points on the imaginary axis.

Theorem 15. *Consider the SISO LTI model (19) characterized by the matrices $\mathcal{A}, \mathcal{B}, \mathcal{C}$. Furthermore, consider the given matrix $S \in \mathbb{R}^{\nu\times\nu}$ with eigenvalues $\sigma(S) = \{s_1, \ldots, s_\nu\}$, the given matrix $L \in \mathbb{R}^{1\times\nu}$ and $\nu < n$. Suppose Assumption 3 holds. Then, for any $\mathcal{G} \in \mathbb{R}^{\nu\times 1}$ such that $\sigma(S) \cap \sigma(S - \mathcal{G}L) = \emptyset$, the reduced-order model (20) with matrices $\mathcal{F} := S - \mathcal{G}L$, $\mathcal{H} := \mathcal{C}\Pi$ with $\Pi \in \mathbb{R}^{n\times\nu}$ the unique solution to the Sylvester equation*

$$\mathcal{A}\Pi + \mathcal{B}L = \Pi S, \tag{21}$$

matches the 0th moments of LTI model (19) at the eigenvalues of S, i.e.,

$$\mathcal{C}(s_i I - \mathcal{A})^{-1}\mathcal{B} = \mathcal{H}(s_i I - \mathcal{F})^{-1}\mathcal{G}, \quad i = 1, \ldots, \nu.$$

Theorem 15 is applied to each of the transfer functions of the LTI part of the Lur'e-type model (2) in order to satisfy constraint (18b). Hereto, we introduce matrices $S_{(i,k)} \in \mathbb{R}^{\nu_{(i,k)}}$ and $L_{(i,k)} \in \mathbb{R}^{1\times\nu_{(i,k)}}$ for $i, k \in \{1, 2\}$. Furthermore, we introduce the notation $\sigma(S_{(i,k)}) \simeq \Omega^0_{(i,k)}$, $i, k \in \{1, 2\}$, meaning that if $0 < \alpha \in \Omega^0_{(i,k)}$, then $\pm j\alpha \in \sigma(S_{(i,k)})$ and if $0 \in \Omega^0_{(i,k)}$, then $0 \in \sigma(S_{(i,k)})$. Loosely speaking, the notation $\sigma(S_{(i,k)}) \simeq \Omega^0_{(i,k)}$, $i, k \in \{1, 2\}$, ensures that the interpolation frequencies in $\Omega^0_{(i,k)}$ are excited by the signal generator. Using this notation, constraint (18b) is satisfied by the results presented in the next theorem.

Theorem 16. *Consider the LTI part of the Lur'e-type model (2) characterized by matrices A, B_1, B_2, C_1, C_2. Consider the given sets of frequencies $\Omega^0_{(i,k)} \in \mathbb{R}^{\eta(i,k)}$ and matrices $S_{(i,k)} \in \mathbb{R}^{\nu_{(i,k)}\times\nu_{(i,k)}}$, $L_{(i,k)} \in \mathbb{R}^{1\times\nu_{(i,k)}}$, $i, k \in \{1, 2\}$, and suppose that $\sigma(S_{(i,k)}) \simeq \Omega^0_{(i,k)}$, $i, k \in \{1, 2\}$. Furthermore, suppose all pairs $(S_{(i,k)}, L_{(i,k)})$, $i, k \in \{1, 2\}$, satisfy Assumption 3. For each $i, k \in \{1, 2\}$, application of Theorem 15 with $(\mathcal{A}, \mathcal{B}, \mathcal{C}) = (A, B_i, C_k)$ and $(S, L) = (S_{(i,k)}, L_{(i,k)})$ results in an LTI model of the form (20) with matrices*

$$\begin{aligned}\left(F_{(i,k)}, G_{(i,k)}, H_{(i,k)}\right) &:= (\mathcal{F}, \mathcal{G}, \mathcal{H}) \\ &= \left(S_{(i,k)} - G_{(i,k)}L_{(i,k)}, G_{(i,k)}, C_k\Pi_{(i,k)}\right).\end{aligned} \tag{22}$$

Then, under the conditions that $G_{(i,k)} \in \Theta_{(i,k)}$, $i, k \in \{1, 2\}$, with

$$\begin{aligned}\Theta_{(i,k)} := \Big\{ &G_{(i,k)} \in \mathbb{R}^{\nu_{(i,k)}} \text{ such that} \\ &\sigma\left(S_{(i,k)}\right) \cap \sigma\left(S_{(i,k)} - G_{(i,k)}L_{(i,k)}\right) = \emptyset \Big\},\end{aligned} \tag{23}$$

the LTI part of the Lure'-type model (3) characterized by the matrices

$$F = \text{blockdiag}\left(F_{(1,1)}, F_{(1,2)}, F_{(2,1)}, F_{(2,2)}\right), \tag{24a}$$

$$G_1 = \begin{bmatrix} G_{(1,1)} \\ 0 \\ G_{(2,1)} \\ 0 \end{bmatrix}, \quad G_2 = \begin{bmatrix} 0 \\ G_{(1,2)} \\ 0 \\ G_{(2,2)} \end{bmatrix}, \tag{24b}$$

$$H_1 = \begin{bmatrix} H_{(1,1)} & H_{(1,2)} & 0 & 0 \end{bmatrix}, \tag{24c}$$

$$H_2 = \begin{bmatrix} 0 & 0 & H_{(2,1)} & H_{(2,2)} \end{bmatrix}, \tag{24d}$$

ensures that $\Upsilon_{(i,k)}(j\omega) = 0$ for $\omega \in \Omega^0_{(i,k)}$, $i, k \in \{1, 2\}$. Hence, constraint (18b) of Problem 13 is satisfied.

Proof. The FRFs (14) of the LTI part of the Lur'e-type model (3) with model matrices (24) reads as follows:

$$\Gamma_{(i,k)} = H_{(i,k)}\left(j\omega I - F_{(i,k)}\right)^{-1} G_{(i,k)},\, i, k \in \{1, 2\}.$$

For each $i, k \in \{1, 2\}$, by Theorem 15, a match is ensured between $\Gamma_{(i,k)}(s)$ and the FRF of the full-order model $\Phi_{(i,k)}(s)$, for all $s \in \sigma(S_{(i,k)})$ if condition (23) holds, i.e., $\Upsilon_{(i,k)}(s) = 0$ for all $s \in \sigma(S_{(i,k)})$. Since $\sigma(S_{(i,k)}) \simeq \Omega^0_{(i,k)}$, $i, k \in \{1, 2\}$, we can conclude that $\Upsilon_{(i,k)}(s) = 0$, $i, k \in \{1, 2\}$ for all $s \in \sigma(S_{(i,k)})$, hence constraint (18b) of Problem 13 is satisfied. ■

Theorem 16 presents the matrices of the LTI block of a family of Lur'e-type models of the form (3) that satisfy constraint (18b). The family is parametrized by $G_{(i,k)} \in \Theta_{(i,k)}, i, k \in \{1, 2\}$. In the next section, we present a method to find $G_{(i,k)} \in \Theta_{(i,k)}, i, k \in \{1, 2\}$, such that the remaining constraints (18c)–(18e) are also satisfied, while (18a) is minimized.

Remark 17. The diagonal structure of the model matrix F in (24a) leaves the dynamics decoupled between the four transfer functions of the LTI block. A negative consequence is that when a match is desired in all FRFs at the same frequency, then that same frequency should be included in all $\Omega^0_{(i,k)}, i, k \in \{1, 2\}$, which results in a reduced-order model with a larger-than-needed state dimension. As a remedy, one could apply moment matching for multi-input, multi-output (MIMO) models, see Shakib, Scarciotti, Pogromsky, Pavlov, and van de Wouw (2023), since the LTI part of the Lur'e-type model is of MIMO nature. However, current moment matching techniques only allow for moment matching along the so-called tangential directions (Antoulas, 2005; Benner, Gugercin, & Willcox, 2015; Gugercin, Antoulas, & Beattie, 2008). As a consequence, not the individual FRFs are matched, but rather their weighted sum, which is undesired in the scope of this work as it does not allow for a straightforward frequency-domain interpretation in terms of the four individual FRFs.

3.1.2. Constrained gradient-based optimization

Let us denote $\theta := \{G^{(1,1)}, G^{(1,2)}, G^{(2,1)}, G^{(2,2)}\}$, which contains all to-be-optimized parameters. We note that the parameters θ only appear in the matrix F, G_1, and G_2, see (24). Therefore, from here on, we write $F(\theta)$, $G_1(\theta)$ and $G_2(\theta)$ to make their dependency on θ clear. Next, we define $\hat{J}$ as follows:

$$\hat{J}(\theta) := J(F(\theta), G_1(\theta), G_2(\theta), H_1, H_2) \tag{25}$$

with J as in (17). Besides minimizing $\hat{J}$, we aim to preserve the convergence property, which is encoded in the constraints of the following optimization problem:

$$\hat{\theta} = \arg\min_{\theta \in \bar{\Theta}} \hat{J}(\theta), \tag{26}$$

where $\bar{\Theta}$ is the set of θ defined as follows:

$$\begin{aligned} \bar{\Theta} = \{\theta \in (\mathbb{R}^{\nu(1,1)} \times \mathbb{R}^{\nu(1,2)} \times \mathbb{R}^{\nu(2,1)} \times \mathbb{R}^{\nu(2,2)}) : \\ \exists P = P^\top \succ 0 : \\ PF(\theta)^-_{\gamma^\star} + (F(\theta)^-_{\gamma^\star})^\top P \prec 0, \\ PF(\theta)^+_{\gamma^\star} + (F(\theta)^+_{\gamma^\star})^\top P \prec 0 \} \end{aligned} \tag{27}$$

with $F(\theta)^\pm_{\gamma^\star} := F(\theta) \pm \gamma^\star G_2(\theta) H_1$ and $\gamma^\star$ as in Assumption 4. We note that $\bar{\Theta} \subset \{\Theta^{(1,1)}, \Theta^{(1,2)}, \Theta^{(2,1)}, \Theta^{(2,2)}\}$, i.e., for any $\theta \in \bar{\Theta}$, the condition (23) is satisfied, since satisfaction of (27) guarantees that $\sigma(F(\theta)) \in \mathbb{C}^-$, while $\sigma(S_{(i,k)}) \in \mathbb{C}^0$ by Assumption 3 for all $i, k \in \{1, 2\}$. One could interpret the minimum in (26) as an infimum, for which a numerical solver should then find a sufficiently accurate approximation of that infimum. A drawback of the LMI constraints in (27) is that checking their feasibility is computationally expensive and that current LMI solvers are limited by the size of the LMIs being in the order of hundreds. To enable a more efficient implementation, we note that $\theta \in \bar{\Theta}$ if and only if the constraint (12) holds for the reduced-order model, i.e., $\sup_{\omega \in \mathbb{R}} \left|\Gamma_{(1,2)}(j\omega)\right| < \frac{1}{\gamma^\star}$, which can be checked efficiently using, e.g., the method in Bruinsma and Steinbuch (1990).

The set $\bar{\Theta}$ in (27) is derived from the statements in Theorem 8 and its LMI constraints are linear in P for fixed θ, hence the constraints in $\bar{\Theta}$ are LMIs. Since $\hat{J}$ in (26) is nonlinear in θ, by gradient-based optimization, a local minimum of $\hat{J}$ at $\hat{\theta}$ can be found, which solves the constrained optimization problem (26) and, thereby, also solves the constrained optimization problem (18a)–(18e) in Problem 13. To launch the gradient-based search to solve (26), an initial convergent reduced-order model is required. A method to find such an initial convergent model is addressed next.

3.1.3. Convergent initial reduced-order model

The full-order model satisfies the condition of Theorem 8 by Assumption 4. In particular, condition (11) is equivalent to bounding the $\mathcal{H}_\infty$ norm of the transfer function of the LTI block of (2) from the nonlinearity φ to the output y by the constant $1/\gamma^\star$, see Pavlov et al. (2006), i.e.,

$$\left\| C_1(sI - A)^{-1} B_2 \right\|_\infty < \frac{1}{\gamma^\star}, \tag{28}$$

where the $\mathcal{H}_\infty$-norm is defined for stable models, i.e., $\sigma(A) \in \mathbb{C}^-$, as follows:

$$\left\| C_1(sI - A)^{-1} B_2 \right\|_\infty := \sup_{\omega \in [0,\infty)} |C_1(j\omega I - A)^{-1} B_2|. \tag{29}$$

To guarantee convergence of the reduced-order model, it is required that the $\mathcal{H}_\infty$ norm of the transfer function $\Gamma_{(1,2)}$ is also bounded by the same constant $1/\gamma^\star$. Hereto, the following lemma presents a reduced-order LTI model that achieves moment matching and preserves the $\mathcal{H}_\infty$ norm of the full-order LTI model.

Lemma 18. *Consider the SISO LTI model (19) characterized by the matrices $\mathcal{A}, \mathcal{B}, \mathcal{C}$. Assume that $\sigma(\mathcal{A}) \in \mathbb{C}^-$ and $\left\|\mathcal{C}(sI - \mathcal{A})^{-1}\mathcal{B}\right\|_\infty < 1/\gamma^\star$, implying that there exists a matrix $\bar{P} \succ 0$ such that the LMIs (11) are satisfied for $A = \mathcal{A}, B_2 = \mathcal{B}, C_1 = \mathcal{C}, P = \bar{P}$ and $\gamma = \gamma^\star$. Application of Theorem 15 for any matrix $S \in \mathbb{R}^{\nu \times \nu}$ and matrix $L \in \mathbb{R}^{1 \times \nu}$ that satisfy Assumption 3 results in a reduced-order model that achieves moment matching at $\sigma(S)$. The reduced-order model is of the form (20) with matrices $(\mathcal{F}, \mathcal{G}, \mathcal{H}) = (S - \mathcal{G}L, \mathcal{G}, \mathcal{C}\Pi)$ and Π the solution to the Sylvester equation in (21). Then, for*

$$\mathcal{G} := \left(\Pi^\top \bar{P} \Pi\right)^{-1} \Pi^\top \bar{P} \mathcal{B}, \tag{30}$$

the matrix $\mathcal{F}$ is Hurwitz, i.e., $\sigma(\mathcal{F}) \in \mathbb{C}^-$, and the transfer function of the reduced-order model satisfies

$$\left\| \mathcal{H}(sI - \mathcal{F})^{-1} \mathcal{G} \right\|_\infty < 1/\gamma^\star. \tag{31}$$

Proof. The proof can be found in Appendix A. ■

The following theorem presents an LMI-based method to find a parametrization $\theta^\circ \in \bar{\Theta}$ for the reduced-order model such that all conditions of Theorem 8 are satisfied.

Theorem 19. *Consider the reduced-order Lur'e-type model (3) with matrices (24) and suppose Assumption 4 holds for a certain $\gamma^\star$. If there exist symmetric positive definite matrices $P_{(i,k)} = P^\top_{(i,k)} \succ 0 \in \mathbb{R}^{\nu(i,k) \times \nu(i,k)}$, matrices $X_{(i,k)} \in \mathbb{R}^{\nu(i,k)}$, for $i, k \in \{1, 2\}$, such that the following two LMIs are satisfied:*

$$\mathcal{L}^+_{\gamma^\star} + \left(\mathcal{L}^+_{\gamma^\star}\right)^\top \prec 0 \text{ and } \mathcal{L}^-_{\gamma^\star} + \left(\mathcal{L}^-_{\gamma^\star}\right)^\top \prec 0 \tag{32}$$

with

$$\mathcal{L}^\pm_{\gamma^\star} = \begin{bmatrix} \mathcal{P}_{(1,1)} & 0 & 0 & 0 \\ \pm\gamma^\star X_{(1,2)} H_{(1,1)} & \mathcal{P}_{(1,2)} \pm \gamma^\star \mathcal{X}_{(1,2)} & 0 & 0 \\ 0 & 0 & \mathcal{P}_{(2,1)} & 0 \\ \pm\gamma^\star X_{(2,2)} H_{(1,1)} & \pm\gamma^\star X_{(2,2)} H_{(1,2)} & 0 & \mathcal{P}_{(2,2)} \end{bmatrix}$$

and

$$\mathcal{P}_{(i,k)} = P_{(i,k)} S_{(i,k)} - X_{(i,k)} L_{(i,k)}, \quad i, k \in \{1, 2\},$$

$\mathcal{X}_{(1,2)} = X_{(1,2)} H_{(1,2)}$.

Then, the conditions of Theorem 8 are satisfied for the reduced-order Lur'e-type model (3) with model matrices $G_{(i,k)} = P_{(i,k)}^{-1} X_{(i,k)}$, $i, k \in \{1, 2\}$. Furthermore, condition (23) is satisfied, i.e., $G_{(i,k)} \in \Theta_{(i,k)}$ for $i, k \in \{1, 2\}$. Finally, the set of LMIs (32) is feasible under the stated assumptions.

Proof. The proof can be found in Appendix B. ■

The initial model matrices $G^{\circ}_{(i,k)}$, $i, k \in \{1, 2\}$, found via Theorem 19 and collected in θ°, render the reduced-order Lur'e-type model (3) convergent. Subsequently, θ° is used to launch a gradient-based search to solve the constrained optimization problem (26).

Remark 20. The results of Lemma 18 can be used beyond the scope of finding an initial convergent Lur'e-type model as presented in Theorem 19. For example, these results can be used to compute a $\mathcal{G}$ such that moment matching is achieved for LTI models and the ℓ_2-gain of the full-order model is preserved.

3.2. Solution to the approximate moment matching Problem 9

The solution to Problem 13 has been presented in Section 3.1. This section computes an error bound for the mismatch between the moment of the full-order and reduced-order model, which is used to compute a constant ε such that Problem 9 is solved. Moreover, it is shown that this error bound holds in the more generic case where inputs u are taken from the class of bounded, periodic inputs $L_2(T)$.

Thanks to Assumption 4 and because the reduced-order model is also convergent, a worst-case upper bound on the error between the steady-state outputs $\bar{z}_u$ of the full-order model and $\bar{\zeta}_u$ of the reduced-order model can be formulated. Hereto, the supremum of the mismatch over *all* FRFs is defined as follows:

$$\bar{\Upsilon} := \max_{i,k \in \{1,2\}} \sup_{\omega \in \mathbb{R}} |\Upsilon_{(i,k)}(j\omega)|. \tag{33}$$

Theorem 21. *Consider the full-order model with moment $C_2\pi(\tau)$ and the signal generator (13) with state $\tau(t) \in \mathbb{R}^{\nu}$. Suppose Assumptions 3 and 4 hold for some $\gamma = \gamma^{\star}$. Furthermore, consider the reduced-order model with moment $H_2 p(\tau)$ following from the application of Theorem 16 and the optimization problem (26). Then, the following mismatch between the moments $C_2\pi(\tau)$ and $H_2 p(\tau)$ holds:*

$$\|C_2\pi(\tau) - H_2 p(\tau)\|_{L_2} \leq \bar{\Upsilon}\bar{\gamma}\, \|L\tau\|_{L_2} \tag{34}$$

with

$$\bar{\gamma} := \left(1 + \frac{\gamma_{\rho u}\gamma^{\star}}{1 - \gamma_{\rho\varphi}\gamma^{\star}}\right)\left(1 + \frac{\gamma_{z\varphi}\gamma^{\star}}{1 - \gamma_{y\varphi}\gamma^{\star}}\right)$$

and $\bar{\Upsilon}$ as in (33) and the constants:

$$\gamma_{\rho u} := \sup_{\omega \in \mathbb{R}} |\Gamma_{(1,1)}(j\omega)|, \qquad \gamma_{\rho\varphi} := \sup_{\omega \in \mathbb{R}} |\Gamma_{(1,2)}(j\omega)|,$$
$$\gamma_{z\varphi} := \sup_{\omega \in \mathbb{R}} |\Phi_{(2,2)}(j\omega)|, \qquad \gamma_{y\varphi} := \sup_{\omega \in \mathbb{R}} |\Phi_{(1,2)}(j\omega)|.$$

Thereby, Problem 9 is solved for $\varepsilon := \bar{\Upsilon}\bar{\gamma}$. Moreover, for any $u \in L_2(T)$, the following upper bound on the steady-state output mismatch holds:

$$\left\|\bar{z}_u - \bar{\zeta}_u\right\|_{L_2} \leq \bar{\Upsilon}\bar{\gamma}\, \|u\|_{L_2} =: \mathcal{V}_u. \tag{35}$$

Proof. The proof can be found in Appendix C. ■

The error bounds in Theorem 21 give the essential insight that a small mismatch in the FRFs of the LTI blocks results in a small error since the bounds in (34) and (35) are linear in $\bar{\Upsilon}$. The optimization problem in (18a) aims at minimizing $|\Upsilon_{(i,k)}(j\omega)|^2$ on a discrete frequency grid for ω, for all $i, k \in \{1, 2\}$, thereby, also minimizing $\bar{\Upsilon}$ in (33). The formulated bounds in Theorem 21 are likely to be conservative due to (i) the stability conditions in Theorem 8 being conservative; (ii) the constant $\bar{\Upsilon}$ holding for any input $u(t) \in L_2(T)$; (iii) usage of the worst-case approximation in the derivation of $\gamma^{\star}$; and (iv) usage of the triangular inequality, which is conservative by its definition. Despite some conservatism, the bounds give the valuable insight that the mismatch in time-domain signals remains bounded for arbitrary input functions selected from the space $L_2(T)$. In a more generic setting without a (global) stability assumption, bounded errors cannot be guaranteed for reduced-order nonlinear models obtained by reduction methods that do not impose a stability property on the reduced-order models, including the time-domain moment matching methods in Astolfi (2010) and Scarciotti and Astolfi (2017a, 2017b).

Remark 22. The constant $\bar{\Upsilon}$ can be made smaller by only evaluating the supremum in (33) at the excited frequencies in the corresponding FRF. The constant $\bar{\gamma}$ in (34) and (35) can be made smaller by redefining the constants $\gamma_{\rho u}, \ldots, \gamma_{y\varphi}$ in Theorem 21 such that the supremum is not taken over $\omega \in \mathbb{R}$, but only at the excited frequencies in the corresponding FRF.

3.3. Overview of the reduction method

An overview of the reduction method is presented in Algorithm 1.

Algorithm 1 Model order reduction algorithm

Input: Full-order Lur'e-type model Σ in (2), the constant $\gamma^{\star}$ as in Assumption 4 and the sets of frequencies $\Omega^0_{(i,k)}$, $\Omega^M_{(i,k)}$, $i, k \in \{1, 2\}$.

1: Define the signal generators (S_i, L_i), $i = 1, 2$, in (13) such that $\sigma(S_i) \simeq \Omega^i_0$ and Assumption 3 holds for each pair.
2: For each $i, k \in \{1, 2\}$, compute the matrices $C\Pi_{(i,k)}$ from (21) with $\mathcal{A} = A$, $\mathcal{B} = B_i$, and $\mathcal{C} = C_k$.
3: Define the reduced-order model matrices $F(\theta)$, $G_1(\theta)$, $G_2(\theta)$, H_1, and H_2, as in (24).
4: Compute initial θ° using Theorem 19.
5: Using $\Omega^M_{(i,k)}$, $i, k \in \{1, 2\}$ and θ°, solve the constrained optimization problem (26) to find $\hat{\theta}$.

Output: Reduced-order model Σ_r in (3) with model matrices $F(\hat{\theta})$, $G_1(\hat{\theta})$, $G_2(\hat{\theta})$, H_1, and H_2 as in (24).

4. Case study

4.1. Model of a flexible beam

In this case study,[1] a one-sided clamped flexible beam supported by a one-sided spring is considered, see Fig. 3 for a schematic depiction. The beam has dimensions length × width × height = 2 m × 50 mm × 30 mm and is characterized by its Young's modulus of 200 GPa and density of 7746 kg/m^3. The linear beam dynamics, characterized by partial differential equations, are discretized by the finite-element method on a uniform spatial grid of 200 points, leaving a state dimension of $n = 800$ consisting of position coordinates, velocity coordinates,

[1] Matlab code for this example is available via the following link: https://github.com/FahimShakib/.

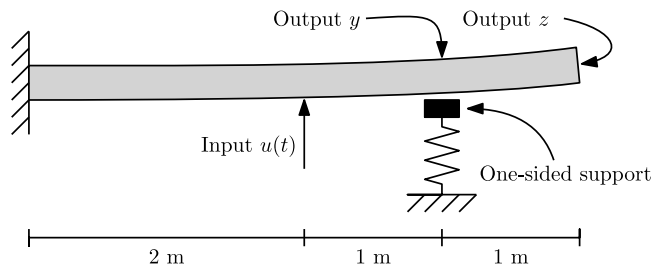

Fig. 3. One-sided clamped flexible beam supported by a one-sided spring.

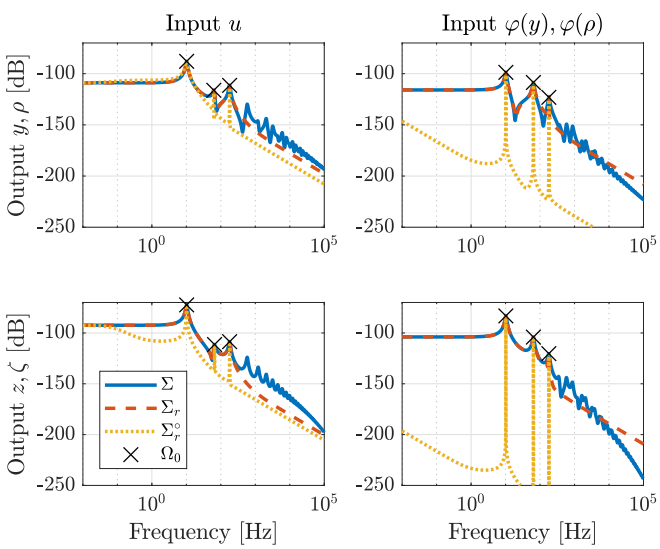

Fig. 4. Bode magnitude diagram of the LTI parts of the Lur'e-type models Σ (full-order model — solid blue), Σ_r (final reduced-order model — dashed red) and Σ_r° (initial reduced-order model — dotted yellow). The interpolation points $\Omega_0^{(i,k)}$, $i, k \in \{1, 2\}$ in (39) are marked by a cross (the interpolation point at 0 Hz is not visible).

inclination coordinates, and angular velocity coordinates. The beam deflection at the end of the beam is considered as the model output z, see Fig. 3. Furthermore, the output y is considered as the deflection of the beam at the location of the one-sided spring. Moreover, an external disturbance $u(t)$ acts in the middle of the beam. The Bode magnitude diagram of the LTI part of the full-order LTI model is depicted in the solid blue curve in Fig. 4. The one-sided spring is modeled as

$$\varphi(y) = \gamma \max(0, y) \tag{36}$$

with stiffness $\gamma = 7.3 \cdot 10^5$, which is also the maximum slope of the nonlinearity. The model is cast in the Lur'e-type form of (2) and is denoted by Σ. The conditions of Theorem 8 are satisfied for the aforementioned γ, which guarantees that the full-order model is convergent.

The goal of this example is to use the reduction method described in Algorithm 1 to find a reduced-order Lur'e-type model that approximates the moment of the full-order Lur'e-type model. Furthermore, the method in Scarciotti and Astolfi (2017b) for generic nonlinear models is also applied, which does not enforce any type of model stability. The two models allow comparing the steady-state mismatch between the model responses for different disturbance situations.

4.2. Moment matching for generic nonlinear models

In this subsection, we demonstrate the application of the method in Scarciotti and Astolfi (2017b). Consider a linear harmonic oscillator $s(\tau) = S\tau, S \in \mathbb{R}^{\nu\times\nu}, \sigma(S) \in \mathbb{C}^0$, and $l(\tau) = L\tau, L \in \mathbb{R}^{1\times\nu}$. A linear signal generator in combination with a function $\delta(\xi) = G \in \mathbb{R}^\nu$ (i.e., independent of ξ) results in the reduced-order dynamics of Wiener form:

$$\begin{aligned} \dot{\xi} &= (S - GL)\xi + Gu, \\ \psi &= h(\pi(\xi)), \end{aligned} \tag{37}$$

where the ξ-dynamics are linear and the model output ψ is a static nonlinear map of the state, see Scarciotti and Astolfi (2017b). Under the assumption that the pair (S, L) is observable, the eigenvalues of $(S - GL)$ can be placed at any desired location in $\mathbb{C}^-$ by a suitable $G \in \mathbb{R}^\nu$. The eigenvalues of $(S - GL)$ being located in $\mathbb{C}^-$ guarantees that model (37) is convergent.

The signal generator is characterized by the following pair (S, L):

$$\begin{aligned} S &= \pi \begin{bmatrix} 0 & 0 & 0 & 0 & 0 & 0 & 0 \\ 0 & 0 & 20.4 & 0 & 0 & 0 & 0 \\ 0 & -20.4 & 0 & 0 & 0 & 0 & 0 \\ 0 & 0 & 0 & 0 & 125.2 & 0 & 0 \\ 0 & 0 & 0 & -125.2 & 0 & 0 & 0 \\ 0 & 0 & 0 & 0 & 0 & 0 & 360 \\ 0 & 0 & 0 & 0 & 0 & -360 & 0 \end{bmatrix}, \\ L &= \begin{bmatrix} 1 & 1 & 0 & 1 & 0 & 1 & 0 \end{bmatrix}, \end{aligned} \tag{38}$$

and the initial condition $\tau(0) = L^\top$. This pair of (S, L) satisfies the conditions of Assumption 1 and corresponds to the interpolation points $s = 2\pi \cdot \{0, \pm 10.2j, \pm 62.6j, \pm 180j\}$, yielding a state-dimension of 7 for the reduced-order model. The numerical values for G are found by a pole placement procedure that places the poles of the reduced-order dynamics in (37) to a subset of poles of the LTI part of the full-order Lur'e-type model. It is non-trivial to compute the mapping $h \circ \pi$ analytically. Therefore, inspired from Scarciotti and Astolfi (2017b), steady-state data is generated on a uniform time grid by simulation of the full-order model by means of the MTF algorithm, see Pavlov et al. (2013). This data is subsequently used to estimate a mapping between τ and $\bar{z}_u$ using linear least-squares regression, where the estimated mapping is a second-order polynomial in the elements of τ.

The reduced-order model reads as (37) with $h \circ \pi$ replaced by $\widehat{h \circ \pi}$. In the remainder of this section, model (37) is called the reduced-order Wiener model. The performance of the reduced-order Wiener model is presented in Section 4.4.

4.3. Moment matching for Lur'e-type models

In this subsection, the application of Algorithm 1 for Lur'e-type models is demonstrated. The following interpolation points for the reduction of the LTI part are selected:

$$\begin{aligned} \Omega_0^{(1,1)} &= \begin{bmatrix} 0 & 10.2 & 62.6 & 180 \end{bmatrix}, \\ \Omega_0^{(1,2)} &= \begin{bmatrix} 0 & 10.2 & 64.1 & 180 \end{bmatrix}, \\ \Omega_0^{(2,1)} &= \begin{bmatrix} 0 & 10.2 & 65.7 & 180 \end{bmatrix}, \\ \Omega_0^{(2,2)} &= \begin{bmatrix} 0 & 10.2 & 64.1 & 180 \end{bmatrix}. \end{aligned} \tag{39}$$

The selected frequencies imply a match of the respective FRF at 0-Hz and at the first three largest resonance peaks, see Fig. 4 where the interpolation frequencies are marked by crosses. Subsequently, the matrices $(S^{(i,k)}, L^{(i,k)})$, $i, k \in \{1, 2\}$, are defined as follows:

$$\begin{aligned} S^{(i,k)} &:= \text{blockdiag}\left(0, \Xi_2^{(i,k)}, \ldots, \Xi_{\eta^{(i,k)}}^{(i,k)}\right), \\ \Xi_\ell^{(i,k)} &:= \begin{bmatrix} 0 & \omega_\ell^{(i,k)} \cdot 2\pi \\ -\omega_\ell^{(i,k)} \cdot 2\pi & 0 \end{bmatrix}, \\ L^{(i,k)} &:= \begin{bmatrix} 1 & 1 & 0 & \ldots & 1 & 0 \end{bmatrix} \in \mathbb{R}^{1\times\nu^{(i,k)}}, \end{aligned} \tag{40}$$

where $\omega_k^{(i,k)}$ is the kth element of $\Omega_0^{(i,k)} \in \mathbb{R}^{\eta^{(i,k)}}$. Assumption 3 holds for all pairs and $\sigma(S^{(i,k)}) \simeq \Omega_0^{(i,k)}$, $i, k \in \{1, 2\}$. Based on the number of interpolation points, it can be concluded that the state dimension of the reduced-order model is 28. Note that the state dimension of the reduced-order Lur'e-type model is four times larger than the state dimension of the reduced-order Wiener model presented in Section 4.2.

The LMIs in Theorem 19 are solved to obtain θ°, that, together with (24), constitute the initial convergent reduced-order Lur'e-type model Σ_r° in (3). The Bode magnitude diagram of Σ_r° is shown in Fig. 4 in the dotted yellow curve. It can be observed that the respective FRFs of the LTI part of Σ and Σ_r° match at the corresponding interpolation points in (39), i.e., constraint (18b) is satisfied. However, for other frequencies, there is a significant mismatch.

Consider the sets $\Omega_M^{(i,k)} = 2\pi \cdot 10^\kappa =: \Omega_M, \kappa \in \mathbb{R}^M$, with $M = 1000$ linearly spaced elements between -2 and 5, implying that elements of the set Ω_M are logarithmically spaced between 0.01 Hz and 10 kHz. Next, the constrained optimization problem (26) is solved in less than 60 s (on an Intel Core i7-7700HQ, 2.8 GHz processor), starting from the initial parameter vector θ°. The resulting $\hat{\theta}$ defines the (final) convergent reduced-order Lur'e-type model Σ_r in (3). The Bode magnitude plot of the LTI part of Σ_r is depicted in the dashed red curve in Fig. 4. With respect to Σ_r°, a significant improvement of the fit of Σ_r to Σ can be observed at almost all frequencies. Furthermore, it can be concluded that an accurate match is obtained up to the frequency corresponding to the third-largest resonance peak. After that frequency, the FRF of the reduced-order model does not match any of the (anti-) resonance peaks.

4.4. Performance of reduced-order models

By means of simulations, the quality of the reduced-order Wiener and Lur'e-type model in terms of approximating the steady-state response of the full-order Lur'e-type model is analyzed. Throughout the rest of this section, $\bar{z}$ is called the steady-state output of the full-order model, $\bar{\zeta}_{Wiener}$ is the steady-state output of the reduced-order Wiener model and $\bar{\zeta}_{Lur'e}$ is the steady-state output of the (final) reduced-order Lur'e-type model.

The steady-state output $\bar{z}$ of the interconnected full-order model (5) with (S, L) in (38) and $\tau(0) = L^\top$ is depicted in Fig. 5, together with the steady-state outputs $\bar{\zeta}_{Wiener}$ and $\bar{\zeta}_{Lur'e}$ of the reduced-order Wiener and Lur'e-type models. It can be observed that the beam deflection is in the order of 100 μm, whereas the approximation error is roughly two orders of magnitude smaller. This concludes that both reduced-order models accurately approximate $\bar{z}$. The same conclusion can be drawn from the column 'Training' of Table 1, where it can be seen that the approximation error in the L_2-norm is roughly three orders of magnitude smaller than the norm of $\bar{z}$. The best approximation is obtained by the reduced-order Lur'e-type model.

To further investigate the accuracy of the reduced-order models, all models are subject to a test with the following two new inputs:

$$u_1(t) = \sum_{k=1}^{10} \sin(2\pi k f_0^1 t), \tag{41a}$$

$$u_2(t) = \sum_{k=1}^{10} \sin(2\pi k f_0^2 t), \tag{41b}$$

where $f_0^1 = 10$ Hz is the base frequency of u_1 and $f_0^2 = 100$ Hz is the base frequency of u_2. The input u_1 excites the beam up to the frequency of 100 Hz, for which an accurate match between

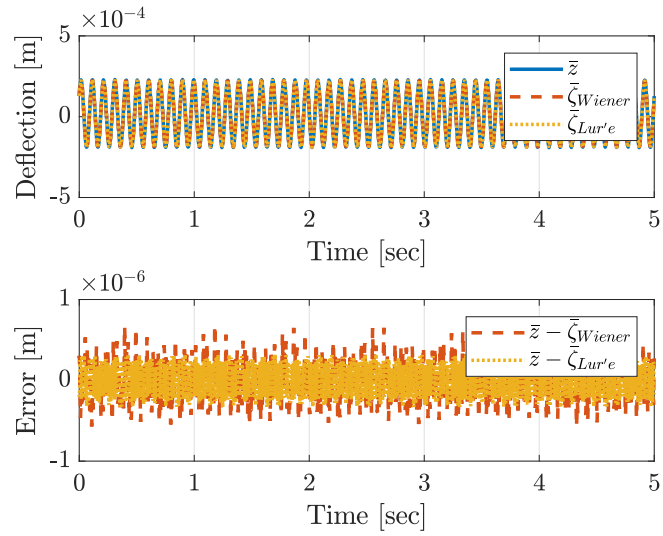

Fig. 5. Top: Steady-state outputs $\bar{z}, \bar{\zeta}_{Wiener}$ and $\bar{\zeta}_{Lur'e}$ subject to the input generated by linear harmonic oscillator characterized by (S, L) in (38). Bottom: Mismatch between the steady-state outputs $\bar{z}$ and $\bar{\zeta}_{Wiener}$ and between outputs $\bar{z}$ and $\bar{\zeta}_{Lur'e}$.

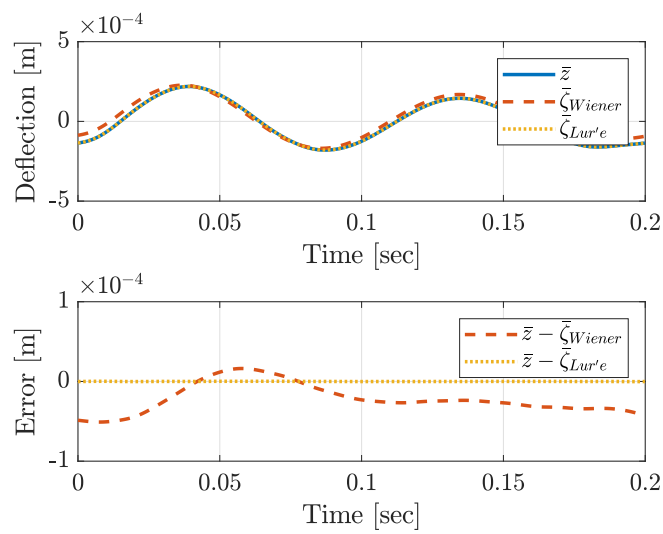

Fig. 6. Top: Steady-state outputs $\bar{z}, \bar{\zeta}_{Wiener}$ and $\bar{\zeta}_{Lur'e}$ subject to input u_1 in (41a). Bottom: Mismatch between the steady-state outputs $\bar{z}$ and $\bar{\zeta}_{Wiener}$ and between outputs $\bar{z}$ and $\bar{\zeta}_{Lur'e}$.

the FRFs of the LTI part of the full-order and reduced-order Lur'e-type model is obtained. The input u_2 excites the beam up to the frequency of 1 kHz, which also excites frequencies for which the match in FRF is not accurate. It can be observed in Fig. 6 that for u_1, the accuracy of the reduced-order Wiener model deteriorated significantly. The accuracy of $\bar{\zeta}_{Lur'e}$, on the other hand, is comparable to the previous test. At this point, it can already be concluded that the reduced-order Lur'e-type model approximates the steady-state output well as long as the input signal excites roughly the same frequencies as those matched in the FRFs. For input u_2, however, the accuracy of the reduced-order Wiener model has a significant mismatch in the 0-Hz component, see Fig. 7. The reduced-order Lur'e-type model, however, approximates the steady-state response of the full-order model reasonably well, even for input signals that contain frequencies for which not a good match is obtained in the FRF. The mismatch

Table 1
Quantitative performance analysis containing the L_2-norm of the output signal $\bar{z}$ and the error signals. The elapsed time for model simulation using the simulation algorithm in Pavlov et al. (2013) is given in the 'Time' columns.

	Training	Time [s]	Validation 1 u_1 (t)	Time [s]	Validation 2 u_2 (t)	Time [s]
$\|\bar{z}\|_{L_2}$	$1.46 \cdot 10^{-4}$	767.75	$1.27 \cdot 10^{-4}$	32.75	$1.30 \cdot 10^{-6}$	3.528
$\left\|\bar{z} - \bar{\zeta}_{Wiener}\right\|_{L_2}$	$2.38 \cdot 10^{-7}$	0.156	$2.84 \cdot 10^{-5}$	0.016	$2.01 \cdot 10^{-5}$	0.098
$\left\|\bar{z} - \bar{\zeta}_{Lur'e}\right\|_{L_2}$	$1.63 \cdot 10^{-7}$	0.776	$1.02 \cdot 10^{-7}$	0.053	$5.27 \cdot 10^{-7}$	0.011
$\mathcal{V}_u$	1.40	–	1.98	–	1.98	–

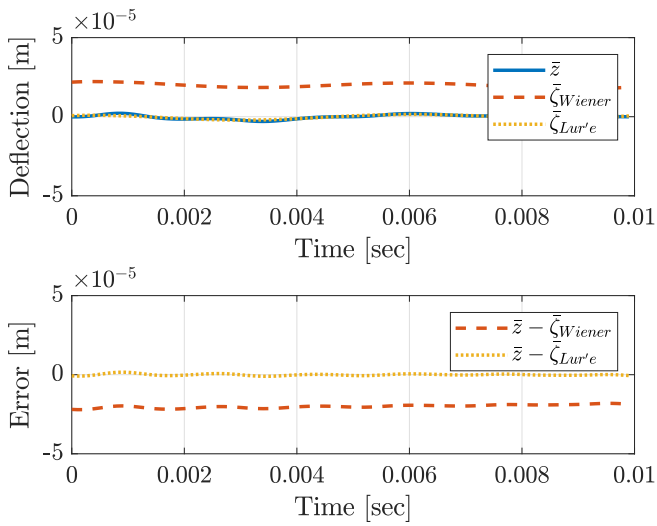

Fig. 7. Top: Steady-state outputs $\bar{z}$, $\bar{\zeta}_{Wiener}$ and $\bar{\zeta}_{Lur'e}$ subject to input u_2 in (41b). Bottom: Mismatch between the steady-state outputs $\bar{z}$ and $\bar{\zeta}_{Wiener}$ and between outputs $\bar{z}$ and $\bar{\zeta}_{Lur'e}$.

is quantified in Table 1, from which the same conclusions can be drawn.

Table 1 includes the upper bound $\mathcal{V}_u$ in (35) for the mismatch $\left\|\bar{z} - \bar{\zeta}_{Lur'e}\right\|_{L_2}$. It can be concluded that this bound is satisfied in all cases and is conservative for this case study. Furthermore, this table includes in the columns 'Time' the elapsed model simulation time using the simulation algorithm in Pavlov et al. (2013). It can be concluded that both the reduced Wiener model and the reduced Lur'e-type model are computationally much cheaper to simulate than the full-order Lur'e-type model.

4.5. Discussion

The case study highlights the benefits of the reduction approach; namely, the reduced-order model preserves the convergence property and provides robustness to input variations. The steady-state mismatch between the response of the full-order and reduced-order Lur'e-type models depends on the quality of the fit in the FRFs. In particular, if the FRFs are fitted accurately over a large frequency range, then the reduced-order Lur'e-type models generally approximate the steady-state output accurately, even though only approximate moment matching (rather than moment matching) is achieved. Such frequency-domain insights are valuable because in many engineering applications use frequency-domain tools for analysis and control design. The model robustness against input variations is generally lacking in other moment matching methods, e.g., the ones in Astolfi (2010) and Scarciotti and Astolfi (2017a, 2017b). However, as explained in Remark 17, the state dimension of the reduced-order model is typically larger than that of the reduced-order models obtained by other moment matching methods (Astolfi, 2010; Scarciotti & Astolfi, 2017a, 2017b) and also the balanced truncation-based methods (Besselink et al., 2011; Padoan et al., 2021). The latter, however, do not guarantee the a priori preservation of the stability property if the reduced-order model dimension is too small. For instance, in the considered case study, the approach in Besselink et al. (2011) can only reduce to order 248 with the guaranteed preservation of the convergence property.

5. Conclusions

This paper proposes a model order reduction technique by time-domain moment matching for Lur'e-type nonlinear models that enjoy the convergence property. The reduction method approximates the moment of the nonlinear model rather than matching it exactly. Preservation of the convergence property of the full-order model guarantees that the reduced-order model exhibits a bounded and asymptotically stable steady-state response for any bounded input and provides robustness against input variations. Furthermore, it allows deriving a bound on the mismatch between the moment of the full-order and reduced-order models. Moreover, the Lur'e-type structure of the model is preserved during reduction, and the characteristic frequency-domain interpretation of moment matching is inherited. In a numerical case study on a one-sided supported beam, the moment of the reduced-order model matches accurately the moment of the full-order model. Furthermore, the reduced-order model also accurately captures the steady-state response to generalized inputs.

Appendix A. Proof of Lemma 18

Proof. The following notation for real square matrices A is used: $\mathrm{He}(A) := A + A^\top$.

The matrix $\mathcal{F} = S - \mathcal{G}L$ is Hurwitz and the inequality in (31) holds if and only if there exists a positive definite matrix Q such that

$$\mathrm{He}\left(Q(S - \mathcal{G}L \pm \gamma^\star \mathcal{G}\mathcal{C}\Pi)\right) \prec 0. \tag{A.1}$$

Let us show that (A.1) holds for the specific choice $\mathcal{G}$ in (30) and $Q := \Pi^\top \bar{P}\Pi$. Note that this choice for matrix Q ensures that it is positive definite, i.e., $Q \succ 0$, since Π is full column rank, see, e.g., Ionescu, Astolfi, and Colaneri (2014). Furthermore, note that $Q\mathcal{G} = \Pi^\top \bar{P}\mathcal{B}$. Substitution of this $\mathcal{G}$ and Q in (A.1) results in:

$$\mathrm{He}\left(\Pi^\top \bar{P}\Pi S - \Pi^\top \bar{P}\mathcal{B}L \pm \gamma^\star \Pi^\top \bar{P}\mathcal{B}\mathcal{C}\Pi\right) \prec 0. \tag{A.2}$$

Note that the Sylvester Eq. (21) can be rewritten as:

$$\mathcal{B}L = \Pi S - \mathcal{A}\Pi, \tag{A.3}$$

which is substituted in (A.2) to yield:

$$\begin{aligned}\mathrm{He}&\left(\Pi^\top \bar{P}\Pi S - \Pi^\top \bar{P}(\Pi S - \mathcal{A}\Pi) \pm \gamma^\star \Pi^\top \bar{P}\mathcal{B}\mathcal{C}\Pi\right)\\ &= \mathrm{He}\left(\Pi^\top \bar{P}\mathcal{A}\Pi \pm \gamma^\star \Pi^\top \bar{P}\mathcal{B}\mathcal{C}\Pi\right)\\ &= \mathrm{He}\left(\Pi^\top \bar{P}\left(\mathcal{A} \pm \gamma^\star \mathcal{B}\mathcal{C}\right)\Pi\right) \prec 0.\end{aligned} \tag{A.4}$$

To show that (A.4) holds, first note that since by assumption $\left\|\mathcal{C}(sI - \mathcal{A})^{-1}\mathcal{B}\right\|_\infty < 1/\gamma^\star$, the following LMIs hold

$$\mathrm{He}\left(\bar{P}(\mathcal{A} \pm \gamma^\star \mathcal{B}\mathcal{C})\right) \prec 0 \tag{A.5}$$

for some positive definite matrix $\bar{P}$. Pre- and post-multiplication of (A.5) with $\Pi^\top$ and Π, respectively, concludes that (A.4) is negative definite (since Π is full column rank). Therefore, we conclude that (31) must hold and that the matrix $\mathcal{F}$ is Hurwitz. The reduced-order model achieves moment matching since $\sigma(\mathcal{F}) \cap \sigma(S) = \emptyset$, guaranteed by $\sigma(\mathcal{F}) \in \mathbb{C}^-$ while $\sigma(S) \in \mathbb{C}^0$ by Assumption 3. ■

Appendix B. Proof of Theorem 19

Proof. We first prove that if the LMIs in (32) are satisfied, then all the conditions of Theorem 8 are satisfied. After that, we prove that there always exists a feasible solution to the LMIs in (32).

Condition (10) is satisfied for the same $\gamma^\star$ as in Assumption 2 thanks to the nonlinear function φ in the reduced-order model (3) being the same nonlinear function as in the full-order model in (2). The LMI condition in (11) with (A, B_2, C_1) replaced by (F, G_2, H_1) in (24), respectively, is equivalent to (11) for $P = \text{blockdiag}(P_{(1,1)}, P_{(1,2)}, P_{(2,1)}, P_{(2,2)})$ and the change of variables $X_{(i,k)} = P_{(i,k)}G_{(i,k)}$, $i, k \in \{1, 2\}$. Thus, the satisfaction of the LMIs (32) is equivalent to satisfaction of the LMIs (11) of Theorem 8. Therefore, satisfaction of the LMIs (32) guarantees that all the reduced-order Lur'e-type model (3) with $G_{(i,k)} = P^{-1}_{(i,k)}X_{(i,k)}$, $i, k \in \{1, 2\}$, satisfies all the conditions of Theorem 8.

Satisfaction of LMIs (11) guarantees that the matrix F is Hurwitz, i.e., $\sigma(F) \in \mathbb{C}^-$, which in turn guarantees that $G_{(i,k)} \in \Theta_{(i,k)}$ for $i, k \in \{1, 2\}$, since $\sigma(S_{(i,k)}) \in \mathbb{C}^0$, which completes this part of the proof.

Finally, we prove the feasibility of the LMI condition in (32). Thanks to the block-triangular structure of $\mathcal{L}^{\pm}_{\gamma^\star}$, for the first $(i, k) = (1, 1)$, third $(i, k) = (2, 1)$ and fourth $(i, k) = (2, 2)$ block diagonal elements, feasibility of (32) is guaranteed if and only if there exists a $G_{(i,k)}$ such that $\sigma(S_{(i,k)} - G_{(i,k)}L_{(i,k)}) \in \mathbb{C}^-$. Such a $G_{(i,k)}$ exists by the observability assumption on the pairs $(S_{(i,k)}, L_{(i,k)})$, $i, k \in \{1, 2\}$. For the second block diagonal element $(i, k) = (1, 2)$, the feasibility of (32) is equivalent to the existence of a $G_{(1,2)}$ such that the $\mathcal{H}_\infty$ norm of the corresponding transfer function is bounded by $1/\gamma^\star$. Hereto, we apply the results of Lemma 18, which shows that there exists a specific $G_{(1,2)}$ such that the $\mathcal{H}_\infty$ norm of the corresponding transfer function is bounded by $1/\gamma^\star$. Since such a $G_{(1,2)}$ exists, we conclude that the LMIs (32) are feasible under the stated assumptions. ■

Appendix C. Proof of Theorem 21

Proof. We start by recalling some inequalities before proving the theorem. For a single-input–single-output LTI model characterized by (A, B, C) and excited by a T-periodic input $u \in L_2(T)$, if the matrix A is Hurwitz, there exists a unique globally exponentially stable T-periodic steady-state solution $\bar{x}_u(t)$ with the corresponding steady-state output $\bar{y}_u$ with $\bar{y}_u \in L_2(T)$. Hence, this model defines a linear operator $g_{yu} : L_2(T) \to L_2(T)$ according to

$$g_{yu}u(t) = \bar{y}_u(t). \tag{C.1}$$

The transfer function of model (A, B, C) from input u to output y reads as $G_{yu}(s) := C(sI - A)^{-1}B, \quad s \in \mathbb{C}$. We recall from Pavlov et al. (2013) that

$$\left\|g_{yu}u\right\|_{L_2} \leq \sup_{m\in\mathbb{Z}} |G_{yu}(jm\omega)| \, \|u\|_{L_2} \leq \gamma_{yu} \, \|u\|_{L_2} \tag{C.2}$$

with $\omega := 2\pi/T$, $\gamma_{yu} := \sup_{\omega\in\mathbb{R}} |G_{yu}(j\omega)|$. For every transfer function of the LTI part of the full-order and reduced-order Lur'e-type model, a linear operator between inputs u, φ and outputs y, z, ρ and ζ can be defined consistent with g_{yu} in (C.1). Then, for any input $u(t) \in L_2(T)$, the following relation holds:

$$\left\|(g_{yu} - g_{\rho u})u(t)\right\|_{L_2} \leq \bar{\Upsilon} \, \|u(t)\|_{L_2}, \tag{C.3}$$

with $\bar{\Upsilon}$ the constant defined in (33). Since $\bar{\Upsilon}$ bounds the mismatch in all $\Upsilon_{(i,k)}$, $i, k \in \{1, 2\}$, similar relations hold also for the other involved FRFs with the same constant $\bar{\Upsilon}$. Furthermore, by the satisfaction of the conditions in Theorem 8 (for both the full-order and reduced-order models), the following bounds hold for signals $\bar{y}(t), \bar{\rho}(t) \in L_2(T)$:

$$\|\varphi(\bar{y}(t)) - \varphi(\bar{\rho}(t))\|_{L_2} \leq \gamma^\star \, \|\bar{y}(t) - \bar{\rho}(t)\|_{L_2}, \tag{C.4a}$$

$$\|\varphi(\bar{y}(t))\|_{L_2} \leq \gamma^\star \, \|\bar{y}(t)\|_{L_2}, \tag{C.4b}$$

where $\gamma^\star$ is the constant in Assumption 4 (incremental sector condition of the nonlinearity). Moreover, satisfaction of the conditions in Theorem 8 guarantees that

$$\gamma^\star\gamma_{y\varphi} < 1 \quad \text{and} \quad \gamma^\star\gamma_{\rho\varphi} < 1 \tag{C.5}$$

with $\gamma_{y\varphi}$ and $\gamma_{y\varphi}$ defined in Theorem 21.

It is shown in this proof that the bound (34) is a special case of the bound (35). Therefore, we prove the latter first and show at the end of the proof that the former is implied. Observe that the steady-state response of the full-order model satisfies

$$\bar{y}(t) = g_{y\varphi}\varphi(\bar{y}(t)) + g_{yu}u(t), \tag{C.6a}$$

$$\bar{z}(t) = g_{z\varphi}\varphi(\bar{y}(t)) + g_{zu}u(t), \tag{C.6b}$$

and that the steady-state response of the reduced-order model satisfies

$$\bar{\rho}(t) = g_{\rho\varphi}\varphi(\bar{\rho}(t)) + g_{\rho u}u(t), \tag{C.7a}$$

$$\bar{\zeta}(t) = g_{\zeta\varphi}\varphi(\bar{\rho}(t)) + g_{\zeta u}u(t). \tag{C.7b}$$

Consider the difference:

$$\begin{aligned}\bar{z}(t) - \bar{\zeta}(t) =& g_{z\varphi}\varphi(\bar{y}(t)) - g_{\zeta\varphi}\varphi(\bar{\rho}(t)) + (g_{zu} - g_{\zeta u})u(t)\\ =& g_{z\varphi}(\varphi(\bar{y}(t)) - \varphi(\bar{\rho}(t)))\\ &+ (g_{z\varphi} - g_{\zeta\varphi})\varphi(\bar{\rho}(t)) + (g_{zu} - g_{\zeta u})u(t).\end{aligned} \tag{C.8}$$

Taking the L_2-norm and using inequalities (C.3) and (C.4a) results in

$$\begin{aligned}\left\|\bar{z}(t) - \bar{\zeta}(t)\right\|_{L_2} \leq& \gamma_{z\varphi}\gamma^\star \, \|\bar{y}(t) - \bar{\rho}(t)\|_{L_2}\\ &+ \bar{\Upsilon}\left(\gamma^\star \, \|\bar{\rho}(t)\|_{L_2} + \|u\|_{L_2}\right)\end{aligned} \tag{C.9}$$

with $\gamma_{z\varphi}$ defined in Theorem 21.

Next we upper bound the terms $\|\bar{y}(t) - \bar{\rho}(t)\|_{L_2}$ and $\|\bar{\rho}(t)\|_{L_2}$. Consider the difference

$$\begin{aligned}\bar{y}(t) - \bar{\rho}(t) =& g_{y\varphi}\varphi(\bar{y}(t)) - g_{\rho\varphi}\varphi(\bar{\rho}(t)) + (g_{yu} - g_{\rho u})u(t)\\ =& g_{y\varphi}(\varphi(\bar{y}(t)) - \varphi(\bar{\rho}(t)))\\ &+ (g_{y\varphi} - g_{\rho\varphi})\varphi(\bar{\rho}(t)) + (g_{yu} - g_{\rho u})u(t).\end{aligned} \tag{C.10}$$

Again, taking the L_2-norm and using inequalities (C.3) and (C.4a) results in

$$\begin{aligned}\|\bar{y}(t) - \bar{\rho}(t)\|_{L_2} \leq& \gamma_{y\varphi}\gamma^\star \, \|\bar{y}(t) - \bar{\rho}(t)\|_{L_2}\\ &+ \bar{\Upsilon}\left(\gamma^\star \, \|\bar{\rho}(t)\|_{L_2} + \|u(t)\|_{L_2}\right),\\ \leq& \frac{\bar{\Upsilon}}{1 - \gamma_{y\varphi}\gamma^\star}\left(\gamma^\star \, \|\bar{\rho}(t)\|_{L_2} + \|u(t)\|_{L_2}\right).\end{aligned} \tag{C.11}$$

The latter step is allowed since $\gamma_{y\varphi}\gamma^\star < 1$ by (C.5). Lastly, using again inequalities (C.3) and (C.4a), we find:

$$\|\bar{\rho}(t)\|_{L_2} = \left\|g_{\rho\varphi}\bar{\varphi}(\rho(t)) + g_{\rho u}u(t)\right\|_{L_2}, \tag{C.12a}$$

$$\leq \gamma_{\rho\varphi}\gamma^\star \|\bar{\rho}(t)\|_{L_2} + \gamma_{\rho u}\|u(t)\|_{L_2}, \tag{C.12b}$$

$$\leq \frac{\gamma_{\rho u}}{1-\gamma_{\rho\varphi}\gamma^\star}\|u(t)\|_{L_2}, \tag{C.12c}$$

where $\gamma_{\rho u}$ is defined in Theorem 21. The latter step is again allowed since $\gamma_{\rho\varphi}\gamma^\star < 1$ by (C.5).

Substitution of (C.12c) into (C.11) and (C.9) and collecting terms yields the bound presented in (35), which completes the proof of the bound (35).

Finally, we show that the bound (34) is a special case of the bound (35). Observe that the moment $C_2\pi(\tau)$ coincides with the steady-state response $\bar{z}_u$ of the full-order model and that the moment $H_2p(\tau)$ coincides with the steady-state response $\bar{\zeta}_u$ of the reduced-order model. Therefore, we can replace the left-hand side of (35) with the left-hand side of (34). Furthermore, substituting $L\tau$ (output of the signal generator) for the input u in (35) results in the bound (34), which completes the proof. ■

References

Antoulas, A. (2005). *Approximation of large-scale dynamical systems*. Philadelphia, USA: SIAM.

Astolfi, A. (2007). A new look at model reduction by moment matching for linear systems. In *Proceedings of the 46th conference on decision and control* (pp. 4361–4366).

Astolfi, A. (2010). Model reduction by moment matching for linear and nonlinear systems. *IEEE Transactions on Automatic Control*, *55*(10), 2321–2336.

Benner, P., Gugercin, S., & Willcox, K. (2015). A survey of projection-based model reduction methods for parametric dynamical systems. *SIAM Review*, *57*(4), 483–531.

Besselink, B., van de Wouw, N., & Nijmeijer, H. (2011). Model reduction for a class of convergent nonlinear systems. *IEEE Transactions on Automatic Control*, *57*(4), 1071–1076.

Besselink, B., van de Wouw, N., & Nijmeijer, H. (2013). Model reduction for nonlinear systems with incremental gain or passivity properties. *Automatica*, *49*(4), 861–872.

Besselink, B., van de Wouw, N., Scherpen, J., & Nijmeijer, H. (2014). Model reduction for nonlinear systems by incremental balanced truncation. *IEEE Transactions on Automatic Control*, *59*(10), 2739–2753. http://dx.doi.org/10.1109/TAC.2014.2326548.

Bruinsma, N., & Steinbuch, M. (1990). A fast algorithm to compute the $\mathcal{H}_\infty$-norm of a transfer function matrix. *Systems & Control Letters*, *14*(4), 287–293.

Gallivan, K., Vandendorpe, A., & Van Dooren, P. (2004). Sylvester equations and projection-based model reduction. *Journal of Computational and Applied Mathematics*, *162*(1), 213–229.

Glover, K. (1984). All optimal Hankel-norm approximations of linear multivariable systems and their L^∞-error bounds. *International Journal of Control*, *39*(6), 1115–1193.

Gugercin, S., Antoulas, A., & Beattie, C. (2008). $\mathcal{H}_2$ Model reduction for large-scale linear dynamical systems. *SIAM Journal on Matrix Analysis and Applications*, *30*(2), 609–638.

Ionescu, T. C., Astolfi, A., & Colaneri, P. (2014). Families of moment matching based, low order approximations for linear systems. *Systems & Control Letters*, *64*, 47–56.

Isidori, A., Sontag, E., & Thoma, M. (1995). *Nonlinear control systems, Vol. 3*. Springer-Verlag London.

Katznelson, Y. (2004). *An introduction to harmonic analysis*. Cambridge: Cambridge University Press.

Kawano, Y. (2021). Controller reduction for nonlinear systems by generalized differential balancing. *IEEE Transactions on Automatic Control*, *67*(11), 5856–5871.

Kawano, Y., & Scherpen, J. (2016). Model reduction by differential balancing based on nonlinear Hankel operators. *IEEE Transactions on Automatic Control*, *62*(7), 3293–3308.

Kawano, Y., & Scherpen, J. (2017). Empirical differential balancing for nonlinear systems. *IFAC-PapersOnLine*, *50*(1), 6326–6331.

Khalil, H. (1996). *Noninear systems*. New Jersey: Prentice-Hall.

Moore, B. (1981). Principal component analysis in linear systems: Controllability, observability, and model reduction. *IEEE Transactions on Automatic Control*, *26*(1), 17–32.

Opdenacker, P. C., & Jonckheere, E. A. (1988). A contraction mapping preserving balanced reduction scheme and its infinity norm error bounds. *IEEE Transactions on Circuits and Systems*, *35*(2), 184–189.

Padoan, A. (2023). Model reduction by least squares moment matching for linear and nonlinear systems. *IEEE Transactions on Automatic Control*, 1–8.

Padoan, A., Forni, F., & Sepulchre, R. (2021). Model reduction of dominant feedback systems. *Automatica*, *130*, Article 109695.

Pavlov, A., Hunnekens, B. G., van de Wouw, N., & Nijmeijer, H. (2013). Steady-state performance optimization for nonlinear control systems of Lur'e type. *Automatica*, *49*(7), 2087–2097.

Pavlov, A., van de Wouw, N., & Nijmeijer, H. (2006). *Uniform output regulation of nonlinear systems: a convergent dynamics approach*. Springer Science & Business Media.

Sarkar, A., & Scherpen, J. (2022). Extended differential balancing for nonlinear dynamical systems. *IEEE Control Systems Letters*, *6*, 3170–3175.

Scarciotti, G., & Astolfi, A. (2017a). Data-driven model reduction by moment matching for linear and nonlinear systems. *Automatica*, *79*, 340–351.

Scarciotti, G., & Astolfi, A. (2017b). Nonlinear model reduction by moment matching. *Foundations and Trends® in Systems and Control*, *4*(3–4), 224–409.

Scarciotti, G., Teel, A., & Astolfi, A. (2017). Model reduction for linear differential inclusions: moment-set and time-variance. In *Proceedings of the 2017 American control conference (ACC)* (pp. 3483–3487). IEEE.

Shakib, M., Scarciotti, G., Pogromsky, A., Pavlov, A., & van de Wouw, N. (2021). Model reduction by moment matching for convergent Lur'e-type models. In *Proceedings of the 2021 American control conference (ACC)* (pp. 4459–4464). IEEE.

Shakib, M., Scarciotti, G., Pogromsky, A., Pavlov, A., & van de Wouw, N. (2023). Time-domain moment matching for multiple-input multiple-output linear time-invariant models. *Automatica*, *152*, Article 110935.

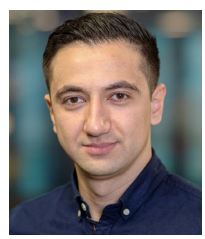

Mohammad Fahim Shakib was born in Herat, Afghanistan, in 1992. He received his M.Sc. degree (cum laude) in Mechanical Engineering from the Eindhoven University of Technology, Eindhoven, the Netherlands in 2017, where he also received his Ph.D. degree (cum laude) in 2022 for his Ph.D. thesis entitled 'Data-driven modeling and complexity reduction for nonlinear systems with stability guarantees'. In 2023, he joined the Control and Power Group, Imperial College London, London, UK, as a Research Associate. His research interests include system identification, model reduction, and control of nonlinear systems.

Giordano Scarciotti (Senior Member, IEEE) was born in Frascati (Rome), Italy, in 1988. He received his B.Sc. and M.Sc. degrees in Automation Engineering from the University of Rome "Tor Vergata", Italy, in 2010 and 2012, respectively. In 2012 he joined the Control and Power Group, Imperial College London, UK, where he obtained a Ph.D. degree in 2016. He also received an M.Sc. in Applied Mathematics from Imperial College in 2020. He is currently a Senior Lecturer in the Control and Power Group. His current research interests are focused on analysis and control of uncertain systems, model reduction and optimal control. He was a visiting scholar at New York University in 2015 and at University of California Santa Barbara in 2016 and a Visiting Fellow of Shanghai University in 2021–2022. He is the recipient of an Imperial College Junior Research Fellowship (2016), of the IET Control & Automation Ph.D. Award (2016), the Eryl Cadwaladr Davies Prize (2017) and an ItalyMadeMe award (2017). He is a member of the EUCA and IEEE CSS Conference Editorial Boards, and of the IFAC and IEEE CSS Technical Committees on Nonlinear Control Systems. He has served in the International Programme Committees of multiple conferences, and he is Associate Editor of Automatica. He was the National Organising Committee (NOC) Chair for the EUCA European Control Conference 2022 and the Invited Session Chair for IFAC Symposium on Nonlinear Control Systems 2022. He is the NOC Chair of the 7th IFAC Conference on Analysis and Control of Nonlinear Dynamics and Chaos 2024.

Alexander Yu. Pogromsky was born in Saint Petersburg, Russia, on March 1, 1970. He received the M.Sc. degree (cum laude) from the Baltic State Technical University, Russia in 1991 and Ph.D. (Candidate of Science) degree from the St.Petersburg Electrotechnical University in 1994. From 1995 till 1997 he was with the Laboratory "Control of Complex Systems" (Institute for Problems of Mechanical Engineering, St. Petersburg, Russia). From 1997 to 1998 he was a research fellow with the Department of Electrical Engineering, division on Automatic Control, Linkoping University, Sweden. In the period of 1999–2001 he was a research fellow with the department

of Electrical Engineering of Eindhoven University and after that he joined the department of Mechanical Engineering of Eindhoven University of Technology, the Netherlands where he works till now. His research interests include theory of nonlinear, adaptive and robust control, nonlinear oscillations.

Alexey Pavlov (born 1976) received M.Sc. degree (cum laude) in applied mathematics from St. Petersburg State University, Russia (1998), and Ph.D. degree in mechanical engineering from Eindhoven University of Technology, The Netherlands (2004). He held various academic and industrial researcher positions at the Institute for Problems of Mechanical Engineering, Russian Academy of Sciences (1999), Ford Research Laboratory, USA (2000), Eindhoven University of Technology (2005), Norwegian University of Science and Technology (2005–2009). From 2009 until 2016 Alexey was a principal researcher in Statoil (now Equinor) Research Centre in Porsgrunn, Norway, working on drilling automation and automatic optimization of oil and gas production. From 2017 until present time Alexey has been a professor in Petroleum Cybernetics at Norwegian University of Science and Technology (NTNU), Department of Geoscience and Petroleum. He is the program manager of BRU21 program – NTNU Research and Innovation Program in Digital and Automation Solutions for the Oil and Gas Industry. He has published the book 'Uniform Output Regulation of Nonlinear Systems: A convergent Dynamics Approach' with N. van de Wouw and H. Nijmeijer (Birkhauser, 2005). He received the IEEE Control Systems Technology Award (2015) "For the development and application of variable-gain control techniques for high-performance motion systems" and IFAC World Congress Best Application Paper Award (2011) for the work "Drilling seeking automatic control solutions". Alexey holds 5 patents and his inventions within automatic optimization are implemented in several oil production fields. His current research interests include control of nonlinear systems, control and optimization of highly uncertain systems, automation and digitalization in energy industry and various industrial applications of automatic control and optimization.

Nathan van de Wouw obtained his M.Sc.-degree (with honours) and Ph.D.-degree in Mechanical Engineering from the Eindhoven University of Technology, the Netherlands, in 1994 and 1999, respectively. He currently holds a full professor position at the Mechanical Engineering Department of the Eindhoven University of Technology, the Netherlands. Nathan van de Wouw also holds an adjunct full professor position at the University of Minnesota, U.S.A. He has been working at Philips Applied Technologies, The Netherlands, in 2000 and at the Netherlands Organisation for Applied Scientific Research, The Netherlands, in 2001. He has been a visiting professor at the University of California Santa Barbara, U.S.A., in 2006/2007, at the University of Melbourne, Australia, in 2009/2010 and at the University of Minnesota, U.S.A., in 2012 and 2013. He has held a (part-time) full professor position the Delft University of Technology, the Netherlands, from 2015–2019. He has published the books 'Uniform Output Regulation of Nonlinear Systems: A convergent Dynamics Approach' with A.V. Pavlov and H. Nijmeijer (Birkhauser, 2005) and 'Stability and Convergence of Mechanical Systems with Unilateral Constraints' with R.I. Leine Springer-Verlag, 2008). In 2015, he received the IEEE Control Systems Technology Award 'For the development and application of variable-gain control techniques for high-performance motion systems'. He is an IEEE Fellow for his contributions to hybrid, data-based and networked control.